

Elsevier required licence: © <2020>. This manuscript version is made available under the CC-BY-NC-ND 4.0 license <http://creativecommons.org/licenses/by-nc-nd/4.0/>

The definitive publisher version is available online at

<https://www.sciencedirect.com/science/article/pii/S0168192320300368?via%3Dihub>

1 **Carbon, water and energy fluxes in agricultural systems of** 2 **Australia and New Zealand**

3 **James Cleverly^{1,2*}, Camilla Vote³, Peter Isaac⁴, Cacilia Ewenz^{4,5}, Mahrita Harahap¹,**
4 **Jason Beringer⁶, David I. Campbell⁷, Edoardo Daly⁸, Derek Eamus¹, Liang He⁹, John**
5 **Hunt¹⁰, Peter Grace¹¹, Lindsay B. Hutley¹², Johannes Laubach¹⁰, Malcolm McCaskill¹³,**
6 **David Rowlings¹¹, Susanna Rutledge Jonker^{7,14}, Louis A. Schipper⁷, Ivan Schroder¹⁵,**
7 **Bertrand Teodosio⁸, Qiang Yu^{1,16,17}, Phil R. Ward¹⁸, Jeffrey P. Walker⁸, John A. Webb¹⁹**
8 **and Samantha P. P. Grover²⁰.**

- 9 [1] School of Life Sciences, University of Technology Sydney, Broadway, NSW, 2007, Australia
10 [2] Terrestrial Ecosystem Research Network, School of Life Sciences, University of Technology
11 Sydney, Broadway, NSW, 2007, Australia
12 [3] Graham Centre for Agricultural Innovation, Charles Sturt University, Wagga Wagga, NSW, 2678,
13 Australia
14 [4] TERN Ecosystem Processes/OzFlux central node, Melbourne, VIC 3159, Australia
15 [5] Airborne Research Australia, PO Box 335, Salisbury South, SA, 5106, Australia
16 [6] School of Agriculture and Environment, The University of Western Australia, Crawley, WA, 6020,
17 Australia
18 [7] School of Science and Environmental Research Institute, University of Waikato, Private Bag 3105,
19 Hamilton, New Zealand
20 [8] Department of Civil Engineering, Monash University, Clayton VIC 3800, Australia
21 [9] National Meteorological Center, Beijing 100081, China
22 [10] Manaaki Wenua-Landcare Research, P.O. Box 69040, Lincoln 7640, New Zealand
23 [11] Institute for Future Environments and Science and Engineering Faculty, Queensland University of
24 Technology, Brisbane, QLD, 4000, Australia
25 [12] School of Environment, Research Institute for the Environment and Livelihoods, Charles Darwin
26 University, NT, 0909, Australia
27 [13] Agriculture Victoria Research, 915 Mount Napier Rd, Department of Economic Development,
28 Jobs, Transport and Resources, Hamilton, VIC 3300, Australia

- 29 [14] Current address: National Institute for Public Health and the Environment, Centre for
30 Environmental Quality, PO Box 1, 3720 BA Bilthoven, The Netherlands
- 31 [15] International CCS & CO2CRC, Resources Division, Geoscience Australia, ACT, 2601, Australia
- 32 [16] State Key Laboratory of Soil Erosion and Dryland Farming on the Loess Plateau, Northwest A&F
33 University, Yangling 712100, China
- 34 [17] College of Resources and Environment, University of Chinese Academy of Science, Beijing
35 100049
- 36 [18] CSIRO, Private Bag No 5, Wembley, WA, 6913, Australia
- 37 [19] Department of Ecology, Environment and Evolution, La Trobe University, Bundoora, VIC,
38 Australia
- 39 [20] Applied Chemistry and Environmental Science, RMIT University, Melbourne VIC 3000,
40 Australia
- 41 *Corresponding author

42

43

44 **Abstract**

45 A comprehensive understanding of the effects of agricultural management on climate–crop
46 interactions has yet to emerge. Using a novel wavelet–statistics conjunction approach, we analysed the
47 synchronisation amongst fluxes (net ecosystem exchange NEE, evapotranspiration and sensible heat
48 flux) and seven environmental factors (e.g., air temperature, soil water content) on 19 farm sites across
49 Australia and New Zealand. Irrigation and fertilisation practices improved positive coupling between
50 net ecosystem productivity ($NEP = -NEE$) and evapotranspiration, as hypothesised. Highly intense
51 management tended to protect against heat stress, especially for irrigated crops in dry climates. By
52 contrast, stress avoidance in the vegetation of tropical and hot desert climates was identified by reverse
53 coupling between NEP and sensible heat flux (i.e., increases in NEP were synchronised with decreases
54 in sensible heat flux). Some environmental factors were found to be under management control,
55 whereas others were fixed as constraints at a given location. Irrigated crops in dry climates (e.g.,
56 maize, almonds) showed high predictability of fluxes given only knowledge of fluctuations in climate
57 ($R^2 > 0.78$), and fluxes were nearly as predictable across strongly energy- or water-limited
58 environments ($0.60 < R^2 < 0.89$). However, wavelet regression of environmental conditions on fluxes
59 showed much smaller predictability in response to precipitation pulses ($0.15 < R^2 < 0.55$), where
60 mowing or grazing affected crop phenology ($0.28 < R^2 < 0.59$), and where water and energy
61 limitations were balanced ($0.7 < \text{net radiation/precipitation} < 1.3$; $0.27 < R^2 < 0.36$). By incorporating
62 a temporal component to regression, wavelet–statistics conjunction provides an important step forward
63 for understanding direct ecosystem responses to environmental change, for modelling that
64 understanding, and for quantifying nonstationary, nonlinear processes such as precipitation pulses,
65 which have previously defied quantitative analysis.

66 **key words:** *wavelet-statistics conjunction, eddy covariance, precipitation pulses, irrigation,*
67 *agriculture, environmental variability*

68

Nomenclature

Environmental factors

ϕ	short-term dryness index
ρ_v	absolute humidity (g m^{-3})
θ	soil water content ($\text{m}^3 \text{m}^{-3}$)
D	vapour pressure deficit (kPa)
G	ground heat flux (W m^{-2}), ($\text{MJ m}^{-2} \text{d}^{-1}$)
P	precipitation (mm d^{-1})
q	specific humidity (g g^{-1})
R_n	net radiation (W m^{-2}), ($\text{MJ m}^{-2} \text{d}^{-1}$)
T_a	air temperature ($^{\circ}\text{C}$)
T_s	soil surface temperature ($^{\circ}\text{C}$)

Turbulent fluxes and flux ratios

BR	Bowen ratio
E	evapotranspiration (mm d^{-1})
H	sensible heat flux (W m^{-2}), ($\text{MJ m}^{-2} \text{d}^{-1}$)
NEE	net ecosystem exchange of carbon ($\mu\text{mol m}^{-2} \text{s}^{-1}$), ($\text{gC m}^{-2} \text{d}^{-1}$)
NEP	net ecosystem productivity ($\mu\text{mol m}^{-2} \text{s}^{-1}$), ($\text{gC m}^{-2} \text{d}^{-1}$)
-NEE	net ecosystem productivity (in regression of NEE) ($\mu\text{mol m}^{-2} \text{s}^{-1}$), ($\text{gC m}^{-2} \text{d}^{-1}$)

Wavelets

Ψ	mother wavelet
a_{\max}	timescale of peak coherence (i.e., peaked squared correlation)
CWT	continuous wavelet transform
DWT	discrete wavelet transform

Statistics

α_i	ith component loading
β_i	regression coefficient for the ith component
ε	regression model error
λ_i	ith eigenvalue
r^2	squared correlation, coherence
R^2	coefficient of determination
envPC _i	ith principal component for environmental factors
fluxPC _i	ith principal component for turbulent fluxes
wCCA	wavelet canonical correlation analysis

69 1 Introduction

70 With the required expansion of agriculture necessary for feeding future populations, it is estimated
71 that 10^9 ha of native and unmanaged ecosystems will be transformed into agricultural uses (Khan and
72 Hanjra, 2009). The associated changes in land cover, land use, and thus ecosystem characteristics
73 have well-established effects on the partitioning of energy and mass fluxes at the land surface. Shifts
74 in albedo, physiology and mass and energy balances can affect weather patterns and regional climate
75 as a result of changes in grazing, irrigation or biomass burning (Beringer et al., 2015; Beringer et al.,
76 2011; Jeong et al., 2014; Lara et al., 2017; Lynch et al., 2007; Mueller et al., 2017; Shao et al., 2017;
77 Yang et al., 2017). As a consequence, biogeochemical cycles will likely be altered, including those of
78 water, carbon, energy and nutrients (Beringer et al., 2011; Foley et al., 2005; Lara et al., 2017).
79 Therefore, the transformation of unmanaged landscapes into managed agricultural systems (or vice-
80 versa, as is sometimes the case with reforestation of previously cleared agricultural lands) will alter
81 seasonal and annual biogeochemical cycles from local to global scales (Beringer et al., 2011;
82 Cunningham et al., 2015).

83 Agricultural systems and yield are vulnerable to weather extremes and climate change (He et al.,
84 2014a; He et al., 2018; Jin et al., 2017; Luo et al., 2018; Mallawaarachchi et al., 2017). Drought and
85 heatwave present a risk of crop failure, although damage can be ameliorated through irrigation and
86 associated evaporative cooling (Adamson et al., 2017; Dreccer et al., 2018; Ellis and Albrecht, 2017;
87 Mueller et al., 2017; Rashid et al., 2018). However, too much precipitation can also present a great
88 risk of crop failure, especially when extreme precipitation occurs aseasonally (Ellis and Albrecht,
89 2017). Between these extremes of droughts and flooding rains, mild water stress might not reduce
90 productivity and yield, depending upon the selection and performance of drought-tolerant genotypes
91 (Cai et al., 2017). Furthermore, climate change can have contrasting effects on winter and summer
92 crops (Cammarano and Tian, 2018). There are strong regional differences in the responses of crops
93 and ecosystems to climate (Dreccer et al., 2018; Hao et al., 2018; Raupach et al., 2013), particularly
94 with respect to water- versus energy-limited ecosystems (Akuraju et al., 2017). These regional
95 differences in environmental conditions inform the economic basis of agricultural management
96 decisions (Meier et al., 2017; Regan et al., 2017). As such, there is an urgent need to identify how
97 management practices across regions might affect the response of biogeochemical fluxes to climate
98 and other environmental factors.

99 Agricultural management is intended to ameliorate unfavourable environmental conditions, thus
100 management type and intensity can have a substantive effect on water and carbon dynamics (e.g.,
101 Behtari et al., 2019; Chi et al., 2016; Davis et al., 2010; Kirschbaum et al., 2017; Laubach et al., 2019;
102 Moinet et al., 2019; Orgill et al., 2017; Ratcliffe et al., 2019; Schipper et al., 2019; Waters et al., 2017;
103 Whitehead et al., 2018; Zeeman et al., 2010; Zhou et al., 2017). Moreover, water and carbon cycles of
104 agricultural systems are complex, influenced heavily by location, soil type and management practises
105 such as cultivar selection, tillage, fertiliser application, irrigation, crop rotation and management of
106 residue and wastewater (Drewniak et al., 2015; Thompson et al., 1999; Waldo et al., 2016).
107 Management practices affect soil carbon stocks in a multitude of ways, including through changes to

primary productivity, biomass removal and decomposition (Kirschbaum et al., 2017; Whitehead et al., 2018). Agricultural management practices such as irrigation and grazing have direct and indirect effects on water-use efficiency (productivity / transpiration), evapotranspiration and CO₂ emissions (Kirschbaum et al., 2017; Tallec et al., 2013; Wagle et al., 2017a; Wang et al., 2017). In this study, the effects of management practices on productivity, evaporation and energy fluxes were investigated from across the agricultural sectors of Australia and New Zealand, ranging from grazed rangelands (low-intensity management) to irrigated/fertilised croplands and high-density dairy farms (high-intensity management).

Across Australia and New Zealand, *ca.* 52% of the landscape is managed at varying intensity for food and fibre production (Australian Bureau of Statistics, 2018; Statistics New Zealand, 2015). Agricultural ecosystems in Australia and New Zealand cover a vast range of climate and environmental conditions, from semiarid rangelands to the humid oceanic climate of New Zealand. Continuous measurements of fluxes and climate conditions across this range provides a wealth of information, but a method of statistical inference has yet to emerge which is not confounded by time-series measurements (Hargrove and Pickering, 1992; Murphy et al., 2010). Recently, wavelet-conjunction analysis has laid a firm theoretical framework for statistical inference of time series (Rhif et al., 2019); some examples are wavelet eigenvalue regression (Abry and Didier, 2018), wavelet principal components analysis (Cleverly et al., 2016a) and discrete wavelet multiple linear regression (Guan et al., 2015; He and Guan, 2013; He et al., 2014b). Building on this previous work, we used a novel wavelet–statistics conjunction to evaluate multivariate linear regression relationships between fluxes (net ecosystem exchange of carbon NEE, evapotranspiration E and sensible heat flux H) and environmental factors (e.g., air temperature T_a , specific humidity q , vapour pressure deficit D, soil water content θ , net radiation R_n , soil temperature T_s and ground heat flux G; see nomenclature for a list of factors and symbols). These environmental factors are not independent, thus our approach first included a wavelet–principal components analysis to identify dependencies amongst environmental

factors and account for those interactions in subsequent regression analyses. Relationships between a flux and a principal component can be associated with the full suite of environmental conditions experienced at a site, as defined by the principal component or components which together explain a majority of the variability in a dataset. For example, if fluctuations in T_a and D were synchronised and thus both had large loadings in the same principal component, any relationship between a flux and that principal component during subsequent regression analysis would then be associated with coordinated fluctuations in both T_a and D , each in proportion to its dependence on the other. This proportion would then be relative to each factor's relative, coordinated amplitude and phase (i.e., component loading in principal components analysis), the degree to which their principal component is related to a flux (from regression analysis), and the proportion of the variation which is explained by their principal component (i.e., the eigenvalue of the principal component). This study aims to synthesise the results from eddy covariance measurements in agricultural ecosystems across the OzFlux research network (<http://ozflux.org.au>; (Beringer et al., 2016)) of the Terrestrial Ecosystem Research Network (Cleverly et al., 2019) and additional independent sites to address the following research question:

How do fluxes under different types of management activities (grazed rangelands, dryland farming, irrigated agriculture, and high density grazing with large input requirements) differ in their responses to environmental drivers?

We hypothesised that: (i) coupling amongst fluxes was expected to be similar across sites within a level of management intensity (low, intermediate, high) because carbon and water fluxes will experience greater physiological coupling if management plays a role in ameliorating crop stress; (ii) coupling amongst environmental factors would be weakened by increasingly intense management, due to the divergence of local and regional climate under highly intense management; and (iii) relationships between fluxes and environmental factors would be similar within a level of management intensity (low, intermediate, high) as a result of hypotheses (i) and (ii). In this work, eddy covariance sites will be identified by their FLUXNET code (AU-xxx, NZ-xxx).

158 **2 Agricultural sites description**

159 Nineteen sites in Australia and New Zealand with uninterrupted time series of fluxes and
160 environmental factors during at least one complete growing season were identified for analysis (Table
161 1, Fig. 1). Because uninterrupted time series are required for wavelet analysis, site selection was
162 restricted to those which contained few, small gaps during the peak of the growing season.
163 Agricultural ecosystems were classified by management intensity: low, intermediate and high. Due to
164 restrictions on the distribution of eddy covariance sites, only one or two datasets sometimes exist for a
165 given management practice (e.g., dryland food crops, $n = 1$), thus management intensity categories
166 could not be further divided by specific management practice without losing statistical power and
167 rigour. Management at low to negligible intensity included only Australian grazed rangelands, which
168 are stocked at very low density and are absent of land clearing, irrigation and fertilisation. At the other
169 extreme, sites with highly intense management have been cleared and levelled, although the regular
170 receipt of irrigation and fertilisation was used to define the high-intensity management class, both for
171 crops and for dairy pastures. Management practices at intermediate-intensity sites often included land
172 clearing and nursery support (e.g., planting, initial but not continuing irrigation or fertilisation for
173 promoting establishment only). Sites with moderate-intensity management included improved
174 pasturelands and unirrigated (dryland) crops, either for consumption by people (food crops) or as
175 forage for livestock (forage crops). Food crops are generally harvested at the end of the growing
176 season, whereas forage crops are typically harvested repeatedly throughout the growing season. These
177 19 sites represent common agricultural activities across a wide range of regions and climates; see
178 supplementary information S1 for a detailed description of the agricultural land use at each site.

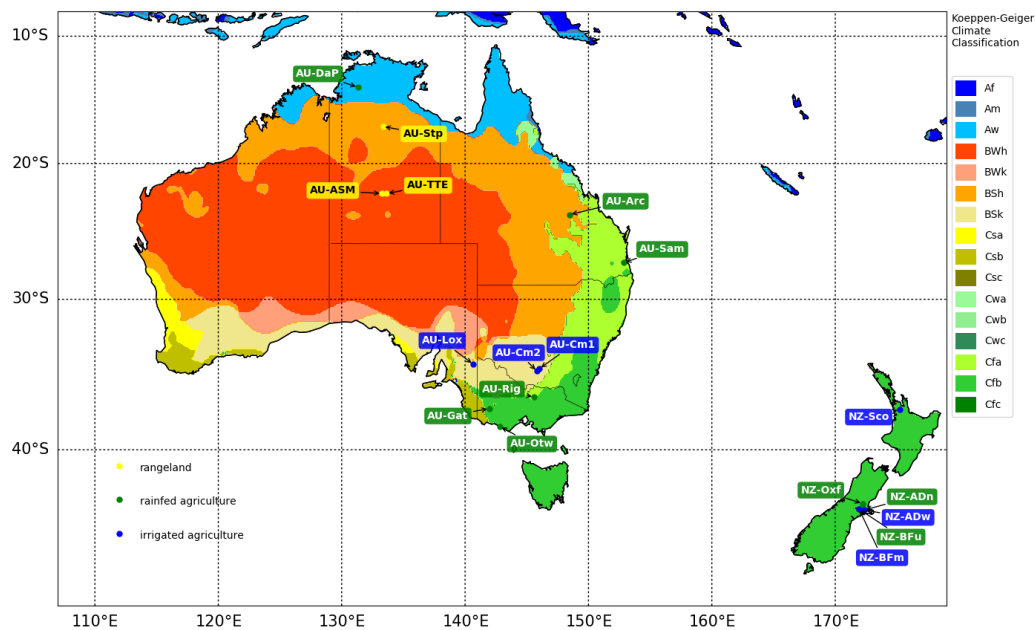


Figure 1. Locations of TERN OzFlux sites used in the analysis and regional Köppen–Geiger climate zones. Sites are categorised by management intensity (rangeland, rainfed agriculture, irrigated agriculture).

179

Table 1. Site details, major land use and management intensity.

Site	Lat/Long	Elevation (m asl)	Dominant vegetation	Major soil type	Temporal coverage	Reference
AU-TTE	-22.29, 133.64	600	Hummock grassland savanna	Red kandasol, drainage sand	Est. 2012	Cleverly et al. (2016c)
AU-ASM	-22.28, 133.25	600	Mulga woodland savanna	Red kandasol	Est. 2010	Cleverly et al. (2013); Eamus et al. (2013)
AU-Stp	-17.15, 133.35	228	Mitchell grassland	Grey vertosol	Est. 2008	Hutley et al. (2011)
AU-Otw	-38.51, 142.80	52	Pasture	Mottled sandy yellow (Sodosol)	2007–2011	Etheridge et al. (2011); Loh et al. (2009)
AU-DaP	-14.06, 131.32	75	Pasture	Red kandasol	2007–2013	Hutley et al. (2011)
NZ-Oxf	-43.26, 172.21	235	Converted paddock	Taitapu Typic Orthic Gley	2005–2010	Brown et al. (2009)
AU-Rig	-36.66, 145.58	152	Pasture	Sodosol	Est. 2010	Beringer et al. (2016)
AU-Gat	-37.39, 141.96	255	Winter pasture	Brown Chromosol/Sodosol	2015–2015	Dresel et al. (2018)
AU-Emr	-23.86, 148.48	170	Chick peas, wheat & pasture	Grey vertosol	2011–2014	Berko et al. (2012)
AU-Sam	-27.39, 152.88	90	Improved pasture	Redoxic hydrosol	Est. 2010	van Delden et al. (2016)

Site	Lat/Long	Elevation (m asl)	Dominant vegetation	Major soil type	Temporal coverage	Reference
NZ-BFu	-43.59, 171.93	204	Kale	Lismore silty loam	2012–2014	Hunt et al. (2016)
NZ-ADn	-43.65, 172.35	34	Lucerne	Stony Balmoral silty loam	Est. 2015	This study
AU-Lox	-34.47, 140.66	36	Almond orchard	Mallee highland (Sodosol)	2008–2009	Stevens et al. (2012)
AU-Cm1	-34.76, 146.02	120	Broadacre crops (maize & wheat)	Transitional red brown earth	2010–2011	Vote et al. (2015)
AU-Cm2	-34.93, 145.82	120	Broadacre crops (rice)	Transitional red brown earth	2010–2011	Vote et al. (2015)
NZ-Sco	-37.77, 175.38	41	Pasture for dairying	Matangi silt loam	Est. 2007	Mudge et al. (2011); Rutledge et al. (2015)
NZ-BFm	-43.59, 171.93	204	Pasture for dairying	Lismore silty loam	2012–2015	Hunt et al. (2016)
NZ-ADw	-43.64, 172.35	33	Lucerne	Stony Balmoral silty loam	Est. 2015	Laubach et al. (2019)

181 To constrain the large range of regional variation across Australia and New Zealand, four sets of co-
 182 located sites were included in this study. The paired grazed-rangeland sites AU-ASM and AU-TTE
 183 were co-located on Pine Hill Cattle station in semiarid central Australia, where grazing pressure ranges
 184 from small in the woodland at AU-ASM (*Acacia* spp.) to negligible in the unpalatable hummock
 185 grasses of AU-TTE (*Triodia schinzii*). Measurements of three "paired" irrigated broadacre crops were
 186 co-located at relatively close proximity in the Coleambally irrigation area (AU-Cm1, AU-Cm2), where
 187 irrigation intensity was highest for rice (*Oryza sativa*), intermediate for summer-season maize (*Zea*
 188 *mays*, also known as corn in some parts of the world), and smallest for wheat (*Triticum sativa*) due to
 189 reduced evaporative demand in the winter. In both sets of paired sites in New Zealand, highly intense
 190 management in the form of irrigation and fertilisation was compared to intermediate-intensity
 191 management for livestock, either as a rainfed forage crop or an intermittently grazed pasture. One pair
 192 of sites was located on Beacon Farm, where the comparison was between irrigated and fertilised
 193 ryegrass (*Lolium perenne*) and clover (*Trifolium repens*) pasture versus rainfed kale (*Brassica*
 194 *oleracea*) (NZ-BFm and NZ-BFu, respectively; Laubach and Hunt, 2018). The second set of paired

195 sites in NZ was at Ashley Dene farm, where the comparison was between an irrigated lucerne
196 (*Medicago sativa*) crop (NZ-ADw), which is also known as alfalfa in some parts of the world, and a
197 rainfed lucerne crop (NZ-ADn).

198 3 Methods

199 3.1 Measurements: eddy covariance and environmental conditions

200 Most of the eddy covariance sites across the OzFlux network use a standard set of instruments,
201 although there is some variation due to site-specific limitations (Isaac et al., 2017). Detailed
202 descriptions of sites, flux tower installation and instrumentation can be found in the references of
203 Table 1. Each EC system was operated at a measurement frequency of 10 or 20 Hz, and fluxes were
204 computed from covariance with vertical wind speed over a 30-minute interval except at AU-Otw,
205 where fluxes were computed hourly. Flux data were processed following Isaac et al. (2017). NEE was
206 assumed to be equal to net carbon flux F_c , where $NEE = F_c = \overline{w'c'}$, w is vertical wind speed, c
207 represents atmospheric carbon dioxide density, primes represent fluctuation around the mean, and the
208 overbar represents a temporal average. Similarly, H was determined as $H = \rho_a C_p \overline{w'T'_a}$, where ρ_a is air
209 density and C_p is the specific heat of air. E was measured as a mass flux $E_{\text{mass}} = \overline{w'\rho'_v}/\rho_w$ and
210 converted to a 30-minute depth equivalent (i.e., converted to units of mm 30-min⁻¹), where ρ_v is
211 absolute humidity and ρ_w is the density of water. Latent heat flux (LE) was determined as the product
212 of L_v and E_{mass} , where L_v is the latent heat of vaporisation and was computed following Stull (1988) as
213 a function of independently measured air temperature (Isaac et al., 2017). See Isaac et al. (2017) for a
214 detailed description of quality control and post-processing procedures used in TERN OzFlux.

215 Because wavelet analysis requires uninterrupted time series, the potential for gapfilling bias is
216 present. Biases introduced during gap filling were minimised by (i) selecting a short analysis period
217 which avoids large gaps (61 days, see §3.2) and (ii) careful screening of each dataset for obvious errors

introduced during gapfilling (e.g., vapour pressure deficit < 0). However, screening came with the potential expense of under-representing agricultural sites in areas of high farm density (cf. Figs. 1 and S1). Gapfilled flux datasets were obtained from <http://data.ozflux.org> or from individual sites. Local optimisation of gapfilling procedures is essential for minimising bias (Isaac et al., 2017), just as local site knowledge is key for providing confidence and consistency in statistical findings (van Gorsel et al., 2018). Wavelet–statistics conjunction could provide a powerful tool for comparing gapfilling approaches (e.g., Moffat et al., 2007), although a complete evaluation of gapfilling procedures should not be limited to agricultural sites and is beyond the scope of the current study.

Gaps in fluxes (NEE, E, H) were filled using either a self-organising linear output (SOLO) model (Eamus et al., 2013; Isaac et al., 2017) or a feed-forward artificial neural network in DINGO (Dynamic INtegrated Gap-filling and partitioning for OzFlux; Beringer et al., 2017) following Moffat et al. (2007). SOLO is an artificial neural network which (Eamus et al., 2013; Hsu et al., 2002): (a) employs a linear statistical kernel, resulting in minimal errors due to over-training; (b) provides access to intermediate products (i.e., SOLO is not a black box type of artificial neural network); and (c) produces small root mean square errors when used for gap filling. Gaps in meteorology were filled using a variety of strategies depending on data availability and suitability, including: SOLO trained on environmental drivers from a paired tower (Cleverly et al., 2016c); linear interpolation for small gaps (≤ 60 minutes); regressions from ancillary data of automatic weather stations operated by the Bureau of Meteorology (in Australia); output from a numerical weather prediction model known as the Australian community climate Earth system simulator (ACCESS); output from the ERA-Interim reanalysis product; or vegetation indices from the moderate resolution imaging spectroradiometer (MODIS) satellite (Isaac et al., 2017). Eight of the datasets used in this study contained no gaps in measurements of environmental factors during the chosen analysis period. Gaps in environmental factors amounted to $0.08 \pm 0.04\%$ of observations across all sites, exclusive of the grazed rangeland AU-Stp where gaps in environmental factors amounted to 35% of the data during the chosen analysis

243 period. Nonetheless, AU-Stp was retained in the analysis to maintain a minimum sample size of three
 244 grazed rangeland sites for analysis in this study.

245 **3.2 Analysis periods**

246 Analysis periods of 61 days were chosen to span the peak of the growing season, defined by
 247 consistently low (i.e., highly negative) values of daytime NEE, but also to minimise overlap with
 248 green-up or senescence periods. Data records for some sites were restricted to a single year,
 249 particularly for those from irrigated broadacre crops (AU-Cm1, AU-Cm2), thus a single growing
 250 season was chosen for evaluation of the 19 sites in the study. Measurements were collected in an
 251 anomalously wet year from AU-Cm1 and AU-Cm2, thus a growing season for sites with multi-year
 252 records was chosen as the most productive year in the record. Differences in climate across sites and
 253 years are important confounding factors for comparisons across the network, and these issues cannot
 254 be ignored. However, a survey of agricultural management conducted from flux measurements
 255 collected simultaneously is impractical, thus we will interpret the results of this study under the
 256 conditions observed during the growing season under analysis (Table 2).

257 **Table 2.** Sixty-one-day analysis period with average (range) of daily fluxes and key environmental conditions for
 258 each site during that period. NEE: net ecosystem exchange of carbon; E: evapotranspiration; H: sensible
 259 heat flux; D: vapour pressure deficit; θ : soil water content; R_n : net radiation; BR: Bowen ratio ($=\Sigma[H]/\Sigma[LE]$;
 260 LE: latent heat flux)

Site	Date range Season	NEE (g m ⁻² d ⁻¹)	E (mm d ⁻¹)	H (MJ m ⁻² d ⁻¹)	D (kPa)	θ (m ³ m ⁻³)	T _a (°C)	R _n (MJ m ⁻² d ⁻¹)	BR (-)
AU-TTE ^a	15/1–17/3/2017	–1.7	3.1	4.7	2.40	0.047	28.4	15.2	0.7
	Summer–Autumn	(–2.0–0.4)	(1.2–4.8)	(0.5–7.3)	(0.93–3.51)	(0.018–0.14)	(22.1–32.1)	(2.1–21.7)	(0.2–1.4)
AU-ASM ^a	15/1–17/3/2011	–0.2	2.8	5.5	1.75	0.092	27.3	15.0	1.3
	Summer–Autumn	(–1.7–2.3)	(0.7–5.1)	(0.9–13.2)	(0.25–4.46)	(0.034–0.26)	(22.8–34.9)	(5.3–19.9)	(0.2–6.5)
AU-Stp	15/2–17/4/2011	–1.9	4.0	2.4	0.98	0.22	25.9	11.9	0.2
	Summer–Autumn	(–4.4–0.1)	(1.5–6.0)	(0.0–4.0)	(0.36–1.82)	(0.11–0.27)	(21.4–28.5)	(2.5–18.5)	(0.0–0.6)

Site	Date range Season	NEE (g m ⁻² d ⁻¹)	E (mm d ⁻¹)	H (MJ m ⁻² d ⁻¹)	D (kPa)	θ (m ³ m ⁻³)	T _a (°C)	R _a (MJ m ⁻² d ⁻¹)	BR (-)
AU-Otw	1/9–31/10/2009	−1.7	1.4	0.2	0.26	0.36	11.1	4.0	1.2
	Spring	(−3.8–2.0)	(0.4–3.3)	(−3.0–2.1)	(0.00–0.7)	(0.22–0.42)	(7.7–21.2)	(0.2–7.5)	(0.2–3.2)
AU-DaP	31/12/2012–2/3/2013	−3.8	4.5	0.7	0.98	0.13	27.8	13.1	0.0
	Wet	(−7.3–0.4)	(1.0–6.2)	(−1.5–3.9)	(0.34–1.65)	(0.061–0.18)	(24.0–31.1)	(1.4–17.8)	(−0.2–0.4)
NZ-Oxf	15/12/2006–14/2/2007	−0.1	1.9	2.0	0.43	0.50	13.5	8.4	1.1
	Summer	(−5.7–4.6)	(0.03–7.7)	(−2.6–5.8)	(0.06–1.57)	(0.46–0.52)	(7.3–21.7)	(−0.4–18.0)	(−17.2–7.5)
AU-Rig	5/6–5/8/2014	−2.3	1.0	−0.3	0.20	0.49	8.6	2.4	0.0
	Winter	(−3.9–0.5)	(0.5–3.1)	(−3.0–2.0)	(0.00–0.51)	(0.38–0.52)	(4.2–13.3)	(−0.8–5.8)	(−1.0–0.7)
AU-Gat	17/8–17/10/2015	−3.2	1.2	1.0	0.51	0.20	11.8	7.1	0.6
	Winter–Spring	(−7.1–2.0)	(0.1–4.0)	(−3.3–6.2)	(0.09–2.38)	(0.10–0.28)	(5.9–23.2)	(1.4–13.0)	(−1.9–3.6)
AU-Emr	5/2–6/4/2012	0.3	1.8	5.0	1.37	0.13	25.3	12.7	1.7
	Summer–Autumn	(−4.4–3.2)	(0.4–4.3)	(0.3–8.1)	(0.22–2.12)	(0.08–0.21)	(21.6–29.3)	(2.9–18.3)	(0.1–6.0)
AU-Sam	15/12/2011–14/2/2012	−2.2	2.4	2.8	0.82	0.51	23.1	12.1	0.5
	Summer	(−4.9–2.4)	(1.1–4.3)	(0.3–5.5)	(0.24–2.41)	(0.39–0.58)	(18.8–28.0)	(3.8–20.1)	(0.1–1.0)
NZ-BFu ^b	19/1–21/3/2014	−2.1	2.3	2.7	0.38	0.15	13.8	9.4	0.5
	Summer–Autumn	(−6.8–4.0)	(0.2–5.3)	(−4.8–8.2)	(0.01–1.60)	(0.11–0.21)	(7.8–20.7)	(−0.4–17.7)	(−1.7–1.8)
NZ-ADn ^c	22/1–24/3/2018	−1.0	2.4	1.8	0.50	0.22	16.3	10.1	0.3
	Summer–Autumn	(−8.5–4.6)	(−0.1–6.5)	(−8.5–7.5)	(0.05–1.52)	(0.10–0.35)	(9.2–24.0)	(1.4–19.2)	(−4.8–1.5)
AU-Lox	11/11/2008–11/1/2009	−6.3	6.5	−1.8	1.35	0.11	20.0	17.3	−0.1
	Spring–Summer	(−9.0–2.2)	(2.8–9.7)	(−10.6–2.8)	(0.36–2.92)	(0.08–0.15)	(11.8–27.4)	(5.3–22.2)	(−0.6–0.2)
AU-Cm1 ^d (Maize)	4/12/2010–3/2/2011	−15.4	5.6	−0.3	1.48	not measured	23.2	18.6	−0.02
	Summer	(−22.9– −1.2)	(2.6–8.0)	(−6.9–3.9)	(0.46–3.45)		(13.9–32.1)	(3.9–23.7)	(−0.4–0.3)
AU-Cm1 ^d (Wheat)	8/8–8/10/2011	−4.9	2.4	0.3	0.76	not measured	16.0	7.1	0.07
	Winter–Spring	(−8.8–0.9)	(0.9–5.1)	(−4.0–3.4)	(0.08–3.02)		(7.4–26.5)	(−0.8–12.2)	(−0.9–0.7)
AU-Cm2 ^d	15/12/2010–14/2/2011	−9.7	5.9	−1.9	1.10	not measured	22.0	21.5	−0.1
	Summer	(−14.7– −1.8)	(3.3–9.5)	(−6.7–1.9)	(0.12–2.64)		(13.4–29.1)	(6.1–27.7)	(−0.4–0.2)
NZ-Sco	15/12/2008–14/2/2009	−2.8	3.7	2.5	0.64	0.42	17.6	14.8	0.3
	Summer	(−7.0–7.3)	(1.1–5.9)	(−0.5–6.2)	(0.25–1.07)	(0.28–0.57)	(14.1–23.3)	(4.1–20.7)	(−0.1–1.3)

Site	Date range Season	NEE (g m ⁻² d ⁻¹)	E (mm d ⁻¹)	H (MJ m ⁻² d ⁻¹)	D (kPa)	θ (m ³ m ⁻³)	T _a (°C)	R _a (MJ m ⁻² d ⁻¹)	BR (-)
NZ-BFm ^b	15/12/2013–14/2/2014	-2.9	3.4	0.5	0.38	0.35	13.9	11.7	0.2
	Summer	(-9.7–3.4)	(0.2–8.0)	(-6.2–5.4)	(0.00–1.54)	(0.22–0.51)	(10.0–20.5)	(1.2–18.7)	(-0.7–1.8)
NZ-ADw ^c	22/1–24/3/2018	-0.7	2.8	0.6	0.45	0.22	16.5	10.1	-1.5
	Summer–Autumn	(-6.4–5.2)	(0.0–8.3)	(-8.9–7.0)	(0.06–1.17)	(0.16–0.27)	(10.2–22.8)	(1.4–19.1)	(-107–2.9)

a, b, c, d paired sites indicated with the same letter

Many of the sites in this study provided a single season of flux data (Table 2), and this was often during a highly productive year like 2010–2011 in Australia (Boening et al., 2012; Cleverly et al., 2016a; Poulter et al., 2014; Xie et al., 2019). Thus to avoid confounding factors of interannual fluctuations in stress and productivity, comparisons in this study were made for each site during its most productive growing season (i.e., the growing season with the lowest daytime NEE). Whereas some sites were highly productive during wet conditions (e.g., irrigated broadacre crops AU-Cm1, AU-Cm2; grazed rangelands AU-ASM, AU-Stp), others were evaluated during drought, including the final year of the Millennium Drought (2009; improved pasture AU-Otw, irrigated almonds AU-Lox), ten years of hydrological drought which generated hardships for irrigated agriculture (Mallawaarachchi et al., 2017; van Dijk et al., 2013), and 2012–2013, the return of drought (improved pasture in the Northern Territory, AU-Dap; rainfed crops and improved pasture in Queensland, AU-Emr and AU-Sam). (Table 2). Climate has continued to fluctuate between extremes of droughts, heatwaves and flooding rains (Cleverly et al., 2016a; Cleverly et al., 2016c; Ma et al., 2016), creating much uncertainty in the agricultural sector (Ellis and Albrecht, 2017). The analysis period for AU-TTE was identified during the return of wet conditions in the summer of 2016–2017, when precipitation in the two months preceding the analysis window (546 mm, 17 Dec 2016–6 February 2017) was similar to that which fell across the entire water year 2010–2011 at AU-TTE's paired site, AU-ASM (565 mm, 1 September 2010–31 August 2011; Cleverly et al., 2016c) (Table 2).

Intense grazing events in New Zealand can strongly increase NEE through enhanced carbon emissions and removal of photosynthetic biomass (Hunt et al., 2016). Thus, analysis periods for flux measurements from New Zealand were either (i) around the peak of the growing season, when high growth rates kept NEE low despite the occurrence of defoliation episodes; or (ii) after conversion to forage crops such as kale (e.g., NZ-BFu).

As an indication of the short-term balance between energy and water limitations on NEE and E, an aridity index value (ϕ) was calculated as $\phi = R_n / (\rho_w L_v P)$ over the analysis period, where ρ_w is the density of water and P is precipitation. Caution is urged regarding the interpretation of ϕ in this study as a short-term measure of ϕ cannot be used to draw inferences of long-term aridity, hydrology or climatology, contrary to the original definition and use of ϕ at an annual timescale (Budyko, 1974). To further characterise site conditions, the Bowen ratio (BR) was also determined as $BR = H/LE$ over the same period.

3.3 Data analysis

A wavelet–statistics conjunction approach was used for all inferences in this study. Time series measurements are an extreme case of the repeated measures experimental design, representing many multiples of repeated observations on an individual experimental unit. This restriction on random sampling creates the possibility of auto-correlation between successive observations, and the presence of this auto-correlation can generate spurious results during statistical inference (Murphy et al., 2010). Such observations are not 'independent and identically distributed' (i.i.d.), leading to misinterpretation of the strength of evidence obtained in statistical analyses (Hargrove and Pickering, 1992). When performing inference between two or more time series, lagged cross-correlation interacts with each pattern of auto-correlation, causing errors due to temporal pseudoreplication (i.e., observations in time which lack independent replication) that are not affected by measurement frequency or persistence of environmental conditions. Thus, time series violate several fundamental assumptions in statistics and

probability theory (e.g., temporal pseudoreplication, auto-correlation, lagged cross-correlation; Hargrove and Pickering, 1992; Murphy et al., 2010). By contrast, the characteristics of wavelet analysis (linearity, localisation in time, energy conservation) make wavelets ideal for statistical inference of time series by interpreting variance in the time series instead of the observations themselves (He and Guan, 2013; He et al., 2014b). This approach invokes the Central Limit Theorem by assuming that auto-correlation in variances is negligible relative to auto-correlation in the observations. Wavelets are finite, cyclic functions that are modulated to identify fluctuations in time and timescale through dilation and translation of a *mother wavelet* (Ψ). Thus, wavelets are ideal for analysis of data with intermittencies or nonstationarities, such as fluxes (Stoy et al., 2005; Stoy et al., 2013; van Gorsel et al., 2013).

A multivariate version of wavelet multiple linear regression (wMLR) was used to infer the relative importance of driving variables on the turbulent fluxes (NEE, E and H). Seven variables were considered as potential drivers of the three fluxes (R_n , T_a , θ , D , q , T_s and G). The complete analysis was performed in three steps: 1) wavelet coherence was used to determine the timescale of peak correlation (a_{\max}) between fluxes and environmental factors, where a_{\max} was used in the following two analyses; 2) wavelet principal components analysis (wPCA; Cleverly et al., 2016a) was performed independently for each site to identify dependencies (i.e., coupling) amongst (i) NEE, E and H (fluxPCs) or (ii) environmental factors (envPCs); and 3) wPCA was combined with wMLR to infer relationships between environmental factors and fluxes (i.e., wavelet canonical correlation analysis, wCCA) at a timescale of a_{\max} .

First (step 1), a_{\max} was identified using wavelet coherence analysis to estimate the correlation between fluxes and environmental factors (Grinsted et al., 2004; Shi et al., 2014; Torrence and Compo, 1998). Fluxes and environmental factors were represented by their main principal components (fluxPCs, envPCs), as described in step (2), except PCs in this step were determined using details at all scales which were supported by the length of a given time series. Coherence between two variables

represents the squared-correlation, r^2 , and wavelet coherence analysis uses a continuous wavelet transformation (CWT) to estimate r^2 . The Morlet wavelet was chosen as Ψ for its functional similarity to turbulence (Cuxart et al., 2002) and its improved compositing (Schaller et al., 2017). Analysis of timescales was limited to 10 scales per octave. Significant coherence was determined using Monte Carlo methods and a red noise auto-regressive null model. Two primary modes of variability were identified, at daily and annual timescales, despite minor differences in coherence across management intensities (Fig. S2). Thus, analyses were performed at a daily timescale.

Next (step 2), dependencies amongst environmental factors were identified using wPCA (Matlab R2013a, The MathWorks Inc., Natick Massachusetts USA). In wPCA, the covariance matrix is populated from the product of paired wavelet coefficients. wPCA is limited to the discrete wavelet transformation (DWT) to simplify construction of the covariance matrix and for computational efficiency. Normalised data were used to account for differences in units amongst environmental factors (equivalent to the use of a correlation matrix as a basis for computation of eigenvalues λ_i and associated eigenvectors). Time series were padded to the next octave j (where the sample size is 2^j) with spectrally neutral values (i.e., the first or last value in the time series) to minimise errors due to the cone of influence. A second-order symlet was chosen for Ψ due to its improved localisation in the frequency domain relative to a first-order 'Haar' wavelet and improved symmetry over the second-order Daubechies wavelet upon which it is based. The resultant linear combinations of environmental factors (X_p) are defined as:

$$\text{envPC}_i = \alpha_{i,1} X_1 + \dots + \alpha_{i,p} X_p, \quad (1)$$

where envPC_i is the i^{th} principal component, α_i is the component loading for envPC_i and p is the number of environmental factors. Similarly, wPCs of the fluxes (fluxPC_i) were determined as $\text{fluxPC}_i = \alpha_{i,\text{NEE}} \text{NEE} + \alpha_{i,\text{E}} \text{E} + \alpha_{i,\text{H}} \text{H}$. Principal components are defined to be orthogonal, meaning they are independent for the purposes of multiple regression analysis (i.e., no colinearity). Principal

components with cumulative eigenvalues ($\lambda_1 + \dots + \lambda_i$) explaining 70% or more of the total variability ($\sum \lambda_p$) were included in following analyses. fluxPC₁ was retained in favour of the original fluxes when its eigenvalue exceeded 70% of the total variability in the fluxes. Variables with a component loading of less than 10% of the total loadings were considered to be independent (i.e., not colinear). wPCA included details for scales 2^1 – 2^x (number of 30-minute periods) and approximations at a scale of 2^x , with x representing the highest integer scale below a_{\max} .

Time series of the principal components were constructed from wPCA-derived loadings α_1 – α_p (e.g., equation 1) and normalised environmental factors or fluxes. A CWT was performed on wPCs to provide samples for wCCA. The Mexican hat wavelet is defined as the second derivative of a Gaussian function (Collineau and Brunet, 1993), and it is effective at locating nonstationarities precisely in time (Schaller et al., 2017). Thus, coefficients from the Mexican hat wavelet represent directional variance by integrating information on timing (Percival and Walden, 2000), validating the application of the Central Limit Theorem and establishing that statistics based upon coefficients from the Mexican hat wavelet represent direct functional responses in one variable to perturbations in another. However, CWT is oversampled, erroneously inflating sample size and degrees of freedom (Katul and Parlange, 1995). Thus, daily-scale variance was computed as the sum of each day's wavelet coefficients. For the Central Limit Theorem to apply, a sample size of at least 30 is required, thus restricting our ability to form rigorous inferences of inter-annual fluxes for sites with a data record which is shorter than 30 years, and this is why daily fluctuations were evaluated in this study.

Initially, the primary mode of variability in the fluxes (fluxPC₁) was regressed against (i) the k number of envPCs which explained a cumulative 70% of the variability in those variables (envPC₁–envPC_k) and (ii) any other environmental factors which contributed less than 10% of the variability to any of envPC₁–envPC_k ($X_a \dots X_n$); for example:

$$\text{fluxPC}_i \sim \beta_{i,0} + \beta_{i,1}X_a + \dots + \beta_{i,n}X_n + \beta_{i,n+1}\text{envPC}_1 + \dots + \beta_{i,n+k}\text{envPC}_k + \beta_{i,n+k+1}X_a \times \dots \times X_n + \varepsilon, \quad (2)$$

where each β is a unique regression coefficient, the term with coefficient β_{n+k+1} is the interaction for X_n non-colinear environmental factors when $n > 1$, and ε is the regression error term.

Next, envPCs which were not significantly related to fluxPC₁ were removed and replaced by any variables which contributed to less than 10% of the variability in the remaining envPCs. In cases where multiple variables were at risk of introducing colinearity in subsequent regression models, each variable which was introduced by removal of an envPC_i was evaluated individually. This is illustrated in the following example, where (i) envPC₂ of two envPCs was not significantly related to fluxPC₁, (ii) all X_1 – X_p contributed more than 10% to the combination of envPC₁ and envPC₂, and (iii) three of X_1 – X_p contribute more than 10% of the variability in envPC₂ but not in envPC₁ (X_x , X_y , X_z):

$$\text{fluxPC}_i \sim \beta_{i,0} + \beta_{i,1}X_x + \beta_2\text{envPC}_1 + \varepsilon, \quad (3a)$$

$$\text{fluxPC}_i \sim \beta_{i,0} + \beta_{i,1}X_y + \beta_2\text{envPC}_1 + \varepsilon \text{ and} \quad (3b)$$

$$\text{fluxPC}_i \sim \beta_{i,0} + \beta_{i,1}X_z + \beta_2\text{envPC}_1 + \varepsilon, \quad (3c)$$

The complete stepwise procedure was repeated for (i) fluxPC₂ or (ii) any of NEE, E or H which represented less than 10% of the loadings on fluxPC₁, wherever either was applicable. The linear importance of each environmental factor for predicting fluxes was estimated from the product of that factor's α in envPC_i and the regression coefficient (β) for that envPC_i, but only if β were significantly different from zero. The importance of each environmental factor for the prediction of fluxes was estimated as $\sum|\beta_{i,X}|$ or $\sum|\alpha_{i,X} \beta_{i,\text{envPC}_i}|$ for significant main effects and envPCs, respectively.

All analyses were performed in Matlab R2018b (The Mathworks, Inc., Natick, Massachusetts, USA), and inferences were based upon a sample size of $N = 61$ days. The probability of a type I error was presumed to be 0.05 ($p < 0.05$) in all hypothesis tests. Because of the nature of wavelet transformation, the equivalent of a multivariate analysis of variance could not be performed. We thus

acknowledge that lacking a single statistical model for all 19 sites increases the probability of an erroneous inference for a site. The coefficient of determination (R^2) for wMLR and wCCA will be distinguished as a capital letter in this study to avoid confusion with coherence or squared correlation, r^2 . Negative statistical coefficients for NEE were taken to indicate increasing values of NEP (NEP = $-NEE$).

All statistical outputs (including those of intermediate steps) and data used in this study can be obtained from the TERN OzFlux data portal (Cleverly, 2019). Example Matlab instructions for data analyses can be found in the Supplementary Material S2.

4 Results

4.1 Management intensity and coupling amongst fluxes

Five combinations of dependencies amongst NEE, E and H were identified across the 19 sites, based upon the sign of their component loadings in wPCA (Table 3).

Table 3. Coupling amongst fluxes from wavelet Principal Components Analysis (wPCA). fluxPC₁: principal component explaining the largest proportion of total variability amongst the fluxes; α : Component loading for NEE (α_1), E (α_2) and H (α_3), respectively. fluxPC1 term not shown for component loadings < 10% of total loadings.

Type	fluxPC ₁	Productivity–E coupling	Productivity–H coupling	E–H coupling	Explanation
Type 1	$\{-\alpha_1 \text{ NEE}, +\alpha_2 \text{ E}, +\alpha_3 \text{ H}\}$	coupled	coupled	coupled	full physiological coupling, no heat stress
Type 2	$\{-\alpha_1 \text{ NEE}, -\alpha_3 \text{ H}\}$	uncoupled	reverse	uncoupled	heat stress, evaporative cooling
Type 3	$\{-\alpha_1 \text{ NEE}, +\alpha_2 \text{ E}, -\alpha_3 \text{ H}\}$	coupled	reverse	reverse	heat stress, isohydric
Type 4	$\{-\alpha_1 \text{ NEE}, -\alpha_2 \text{ E}\}$	reverse	uncoupled	uncoupled	low D, no heat stress
Type 5	$\{-\alpha_1 \text{ NEE}, -\alpha_2 \text{ E}, +\alpha_3 \text{ H}\}$	reverse	coupled	reverse	low D, energy limited

415 Examples of Type 1 dependencies amongst fluxes were found in every management intensity class,
 416 although Type 1 dominated in the highly intense management class (Fig. 2, Table S1). Increases in
 417 NEP were synchronised with increasing E and H (Type 1) at nine locations (Fig. 2).

418 Only Type 1 and Type 2 dependencies were observed in the grazed rangelands of this study. In
 419 Type 2 and Type 3 dependencies, decreasing NEE (i.e., increasing NEP) was synchronised with
 420 decreasing H, indicative of a negative heat stress response. For Type 2, variation in E represented less
 421 than 10% of the total flux variability and was thus considered to be uncoupled from fluctuations in
 422 NEE or H. Type 2 relationships were observed at four rangeland and pasture sites (Fig. 2). Type 3
 423 relationships in which NEP was positively correlated to E and inversely correlated to H occurred on
 424 four of the 19 farms (Fig. 2). Positive coupling with E on the highly managed Ashley Dene Farm (NZ-
 425 ADw) was small in magnitude, comparable to that of Type 2 dependencies on farms with
 426 intermediate-intensity management (Fig. 2). Reverse coupling between NEP and E was uncommon,
 427 observed at only one site for each of Type 4 and Type 5 dependencies. Refer to Table S1 for
 428 individual results from each of the 19 sites.

429 **4.2 Coupling amongst environmental**
 430 **factors**

431 Complete wPCA results for the seven
 432 environmental factors are also provided in
 433 Table S1. Interactions amongst environmental
 434 factors were generally site specific, varying
 435 across sites in the identity and strength of
 436 contributing variables and in the amount of
 437 variation explained by envPCs (Fig. S3). Thus,

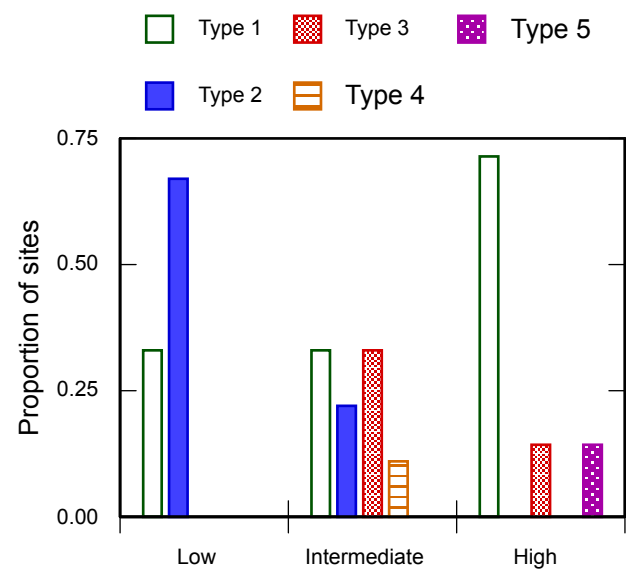


Figure 2. The relative proportion of sites showing each of the wavelet PCA component loading types for fluxes for each management class (low, intermediate, high). Refer to Table 3 for a description of flux coupling types.

dependencies amongst environmental factors were evaluated in detail at the paired sites to minimise differences introduced by the large distances between farms in this study (Fig. 3).

In grazed rangelands, R_n and G maintained similar relationships across Pine Hill Station (AU-ASM, AU-TTE), whereas T_a , T_s , θ and q showed a *ca.* 180° phase shift relative to the R_n – G axis across sites

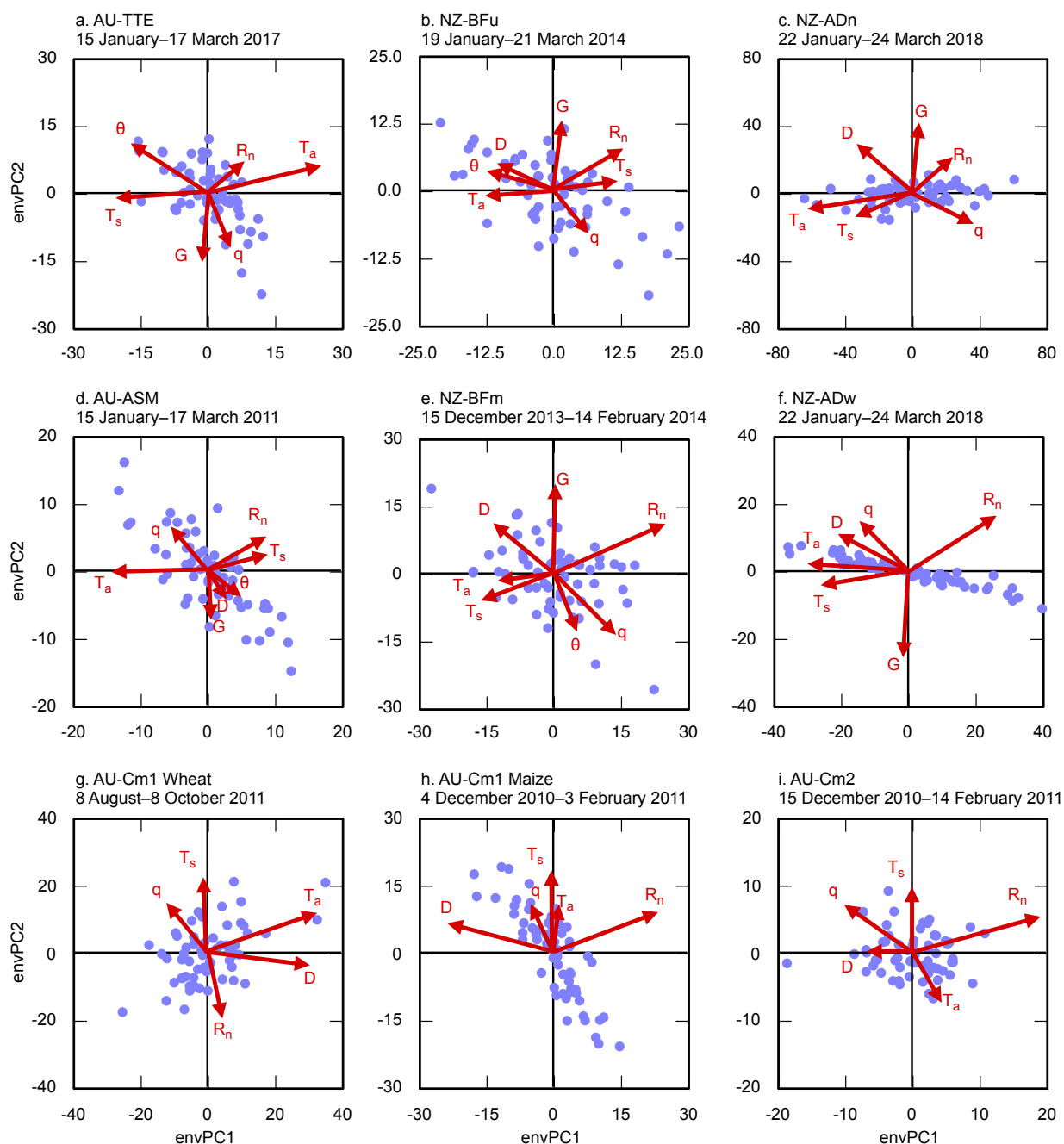


Figure 3. Wavelet PCA at the paired sites. Paired sites were grazed rangeland (a, d; AU-ASM, AU-TTE), irrigated/fertilised dairy pasture (b; NZ-BFm) versus unirrigated/unfertilised forage crop kale (e; NZ-BFu), irrigated/fertilised versus unirrigated/unfertilised forage crop lucerne (c, f; NZ-ADw, NZ-ADn), and irrigated broadacre crops (g, h, i; AU-Cm1 wheat, maize, AU-Cm2 rice).

(Fig. 3a, d). In the comparison of an irrigated and fertilised pasture (NZ-BFu) versus a kale forage crop (NZ-BFm), fluctuations of T_s and θ differed across the two datasets; irrigation and fertilisation induced a shift from coupling of T_s with R_n to coupling of T_s with T_a , and highly intense management induced a shift in coupling for θ from D to q , representing a release of θ from atmospheric water stress (Fig. 3b, e). In lucerne, fluctuations in G and q differed between irrigated and unirrigated paddocks on Ashley Dene farm, whereas relative coupling amongst R_n , D , T_a and T_s were fixed (NZ-ADn, NZ-ADw; Fig. 3c, f). In irrigated broadacre crops of the Coleambally Irrigation Area, fluctuations in T_s and q were similarly correlated in winter (AU-Cm1 wheat) and summer (AU-Cm1 maize, AU-Cm2 rice; Fig. 3g–i). With the exception of D , heavy irrigation for the cultivation of rice created similar relationships amongst environmental factors as irrigated cultivation of wheat during the winter and spring, but T_a dominance in winter (Fig. 3g) was exchanged for R_n dominance in summertime irrigated rice (Fig. 3i). Across all comparisons, some environmental factors maintained the same contribution to total environmental variability at paired sites, whereas other environmental factors were rotated relative to the fixed factors, suggesting that management can influence some environmental factors, but others are beyond management control.

4.3 Management responses of fluxes to environmental factors

R^2 from wCCA for the regression of fluctuations in NEE, E and H against fluctuations in meteorological and edaphic conditions ranged from 0.16 at AU-Emr to 0.88 at AU-Gat (Fig. 4). Values of R^2 in Figure 4 for NEE, E or H which were not different at a given site were obtained from a single wCCA model, and only values of R^2 which were significantly different from zero are presented in Figure 4. Representing predictability of variations in fluxes, R^2 did not show consistent patterns across management intensity classes, but there were some general trends. Grazed rangelands had small R^2 as a group (0.34 ± 0.06), with a range of values (0.17–0.54) which overlapped completely with the range of R^2 values from sites managed at intermediate intensity (0.16–0.88, 0.55 ± 0.07). By

contrast, the range of R^2 for grazed rangelands overlapped only slightly with the range of R^2 from highly intense management (0.42–0.84, 0.62 ± 0.07). Similar to the grazed rangelands, the range of R^2 values for sites with high-intensity management overlapped completely with the range of R^2 values from intermediate-intensity management (Fig. 4). No relationships between R^2 and ϕ were apparent in grazed rangelands (Fig. 4). At sites with intermediate-intensity management, the smallest values of R^2 were observed at intermediate ϕ ($R^2 = 0.28$ – 0.35 ; NZ-ADn, AU-DaP, AU-Otw), with the exception of low R^2 for rainfed crops at AU-Emr ($R^2 = 0.16$). Amongst sites with highly intense management, R^2 was highest in the three irrigated farms with the highest ϕ ($R^2 = 0.78$ – 0.84 ; AU-Lox almonds, AU-Cm1 maize, NZ-Sco dairy; Fig. 4).

In all except three cases, a single inference model was obtained, with only envPCs and factors which were not co-linear with the envPCs explaining fluctuations in NEE, E and H (Table S2, Fig. S3). This indicates that fluxes generally responded to coupled environmental factors instead of individually to those environmental factors. One exception was in irrigated maize (AU-Cm1), where fluctuations in q were co-linear with envPC₂ and not envPC₁, but fluctuations in q alone (amongst the co-linear factors in envPC₂) were significantly related to variation in NEE, E and H ($\beta_q = -0.06 \pm 0.01$, $p < 0.001$) without contributions from other co-linear factors in envPC₂ ($\beta_{\text{envPC}_2} = -0.06 \pm 0.06$, $p = 0.35$) ($R^2 = 0.79$, $p < 0.001$; Fig. 5). This site provides an example of a strong environment–flux

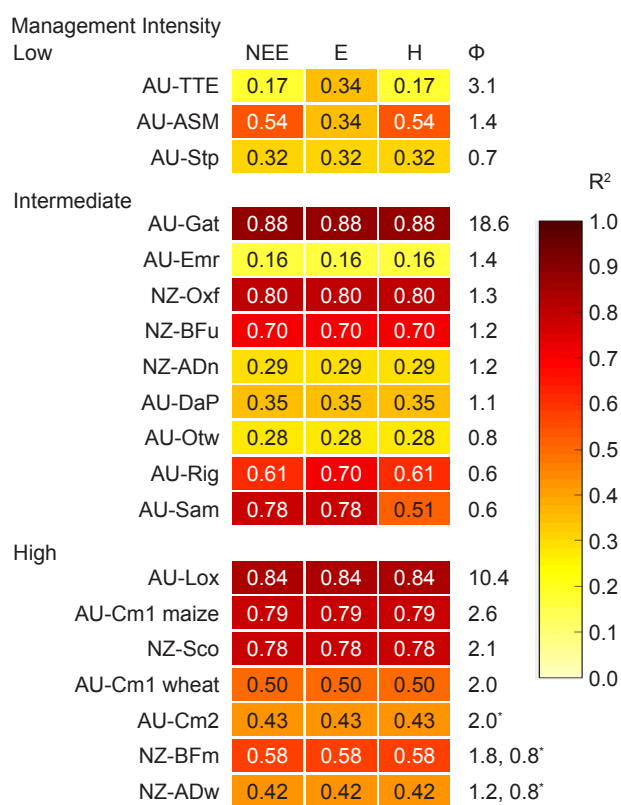


Figure 4. Heat map of coefficients of determination (R^2) from wCCA. Sites are arranged within a management-intensity class according to their short-term aridity index (ϕ). Values of ϕ marked by an asterisk included farm-scale irrigation amounts.

relationship due to both individual factors (q) and interacting environmental factors (R_n and D ; cf. Fig. 5, Table S1).

The improved pasture AU-Otw similarly showed fluctuations in D to contribute to explaining fluctuations in NEE, E and H from outside of $envPC_2$, although strong nonlinearities were present which reduced the strength of statistical inference for all environmental factors at this site ($R^2 = 0.11$ –

0.28 , $p = < 0.001$ – 0.03 ; Table S2, Fig. 6). In this example, the full model with $envPC_1$ and $envPC_2$, along with non-colinear R_n , resulted in no values of β_x which were significantly different from zero (β_{R_n} , β_{envPC_1} and β_{envPC_2} of -0.009 ± 0.04 , -0.15 ± 0.11 and 0.03 ± 0.11 , respectively; Table S2) and a small R^2 which was nonetheless significantly different from zero ($R^2 = 0.11$, $p = 0.02$). This discrepancy was likely induced by nonlinearity in the residuals, particularly near values of zero on the x-axis which represent a large range of fluctuations in NEE, E and H under stable environmental conditions (Fig. 6). D contributed little to $envPC_1$ at this site, so removal of $envPC_2$ from the regression permitted the inclusion of D as a main effect. Doing so resolved the discrepancy between

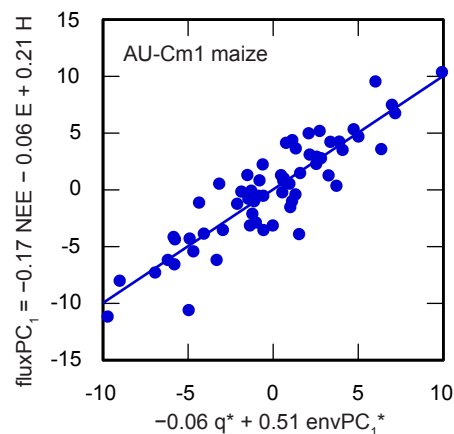


Figure 5. wCCA results for an example irrigated broadacre crop. See supplementary material for details of regression statistics (Table S2, Fig. S1). Asterisks represent factors with coefficients significantly different from zero.

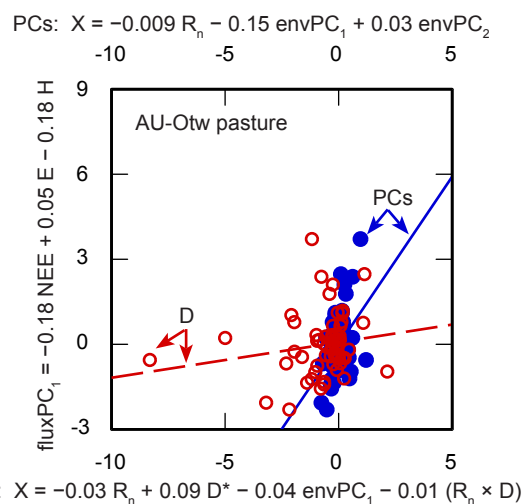


Figure 6. wCCA results for an example improved pasture. See supplementary material for details of regression statistics (Table S2, Fig. S1). 'PCs' statistical model: closed symbols, solid line and top abscissa axis; 'D' model: open circles, dashed line and bottom abscissa. Asterisks represent factors with coefficients significantly different from zero.

515 model and submodel results, showing a weak
 516 linearity in fluxes with respect to fluctuations in
 517 D without losing nonlinear effects near the y-
 518 axis (Fig. 6).

519 Strong nonlinearities were observed at many
 520 sites (Fig. S3), with an example from grazed
 521 rangeland AU-ASM shown in Figure 7. For
 522 fluxPC₁, the response was largely linear ($R^2 =$
 523 0.54), but with notable nonlinearities in the
 524 residuals. This suggests that environment–flux
 525 relationships contain a linear portion and a
 526 nonlinear portion, the latter due to lags in the

527 cycles of perturbation and response (Fig. 7). Nonlinear responses were dominant for E ($R^2 = 0.34$; Fig.
 528 7), suggesting that the sensitivity of E to precipitation pulses is largely independent of climate
 529 conditions in central Australia.

530 No single environmental factor accounted for fluctuations in NEE, E and H, and there was much
 531 variability across sites within each management intensity class (Fig. 8). The most important factors for
 532 explaining linear responses of fluxes in grazed rangelands (importance > 15%) were T_s , T_a and G (0.23
 533 ± 0.11 , 0.19 ± 0.09 and 0.17 ± 0.11 , respectively; Fig. 8). In intermediate-intensity management, most
 534 environmental factors were important for predicting fluxes: T_a , R_n , G and D (0.15 ± 0.02 , 0.12 ± 0.03 ,
 535 0.25 ± 0.08 and 0.17 ± 0.06 , respectively; Fig. 8). Environmental factor importance was similar to
 536 intermediate-management in highly intense management, except that T_a was replaced by θ : θ , R_n , G
 537 and D (0.16 ± 0.05 , 0.20 ± 0.04 , 0.16 ± 0.03 and 0.27 ± 0.11 , respectively; Fig. 8).

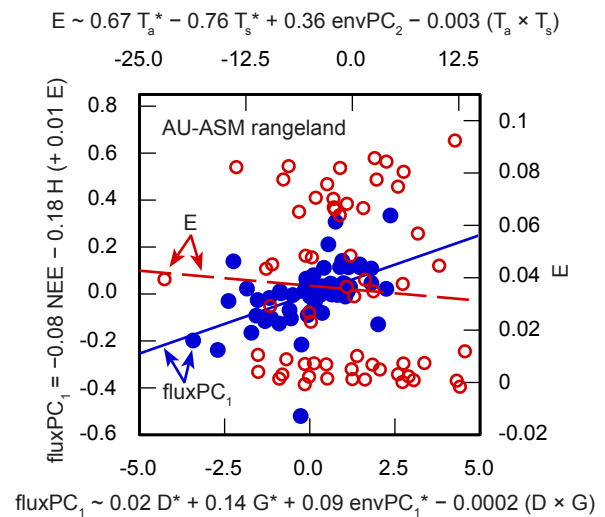


Figure 7. wCCA results for an example and grazed rangeland. See supplementary material for details of regression statistics (Table S2, Fig. S1). 'fluxPC₁': closed circles, solid line, bottom abscissa and left ordinate axes; 'E' in (c): open circles, dashed line, top abscissa and right ordinate. Asterisks represent factors with coefficients significantly different from zero.

538 5 Discussion

539 Simple regression of environmental factors
 540 alone has been previously found to fit measured
 541 fluxes better than the output of land-surface
 542 models, although the reasons for this have not
 543 yet been identified (Best et al., 2015; Haughton
 544 et al., 2018b). Nonetheless, no consensus has
 545 been reached regarding identification of the key
 546 environmental factors driving variations in
 547 surface fluxes, which is still an active area of
 548 inquiry. Thus, a call has been issued for more

549 studies to evaluate climate and management effects using paired and multiple towers (Mudge et al.,
 550 2011). In this study, we used a multivariate wavelet–statistics conjunction approach to evaluate
 551 management effects on relationships between fluctuations in environmental factors and synchronised
 552 fluctuations of carbon, water and heat fluxes (NEE, E and H, respectively). Coupling amongst fluxes
 553 showed some key differences across management intensity categories, providing partial but not
 554 overwhelming support for hypothesis 1. By contrast, coupling amongst environmental factors
 555 appeared to be strongly site-specific and showed inconsistent effects of management in comparison of
 556 paired sites at a single location, thus failing to support our hypothesis that increasingly intense
 557 management would weaken integration of environmental factors (hypothesis 2). Despite site-specific
 558 coupling amongst environmental factors, we found relationships between fluxes and environmental
 559 factors to depend upon management intensity and the short-term level of aridity within a management
 560 intensity class (Fig. 4), providing support for hypothesis 3. However, no single environmental factor
 561 was found which explained variability in fluctuations of NEE, E or H, consistent with previous
 562 findings (Hao et al., 2018); for example, enhanced vegetation index, photosynthetically active

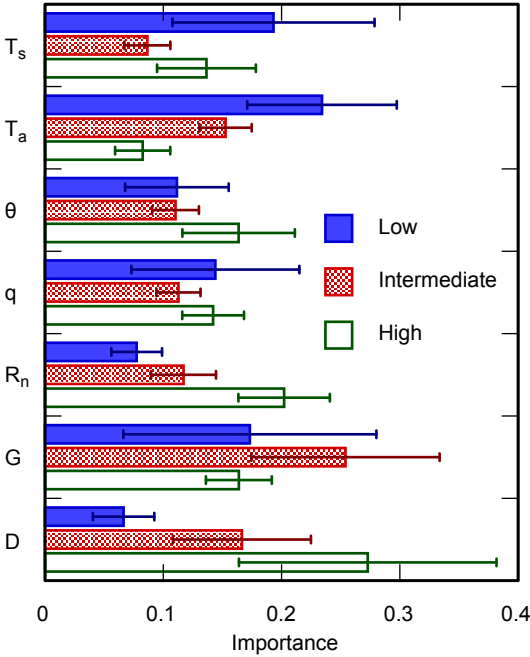


Figure 8. Proportional importance (\pm standard error) of environmental factors in wCCA for each management intensity class (low, intermediate, high).

radiation and air temperature were all found to be significantly correlated to E by Wagle et al. (2017b). Instead, the way in which environmental factors co-varied through time (i.e., their synchronised interaction) affected variations in NEE, E and H, especially in water-limited landscapes where precipitation pulses dominate the coordination of fluxes and environmental factors (Cleverly et al., 2013).

5.1 Coupling of carbon, water and energy cycles

The largest effect of management identified in this study was upon the relationship amongst fluxes. Even though examples of full, positive coupling between NEP, E and H (Type 1, $\{-NEE, +E, +H\}$) were found for each management intensity class in our study (on nine farms), the proportion of sites showing such full coupling increased with increasingly intense management (Fig. 2). Intense management practices like irrigation and fertilisation are intended to minimise the impact of detrimental environmental conditions and maximise yield, thus generating synchronisation amongst carbon, water and energy fluxes. There can be regional variation in the response of crops to heat and water stress (Dreccer et al., 2018), although managing for heat stress can be as simple as converting from dryland agriculture or pasture to irrigated agriculture, if enough water is available. Because many irrigated broadacre cropping and arboreal horticultural systems exist in water-limited climates with high evaporative demand and the potential for plant stress (Stokes et al., 2008; Williams et al., 2002), as they do in the Australian examples of this study, they can require substantial volumes of irrigation water to return a profitable yield. Irrigated almonds in this study (AU-Lox) did not show any apparent stress, with coupling of NEP, E and H. Irrigation can protect against physiological stress and stress-induced crop failure by ameliorating heat extremes through evaporative cooling (Chen et al., 2017; Cleverly et al., 2016b; Cleverly et al., 2015; Stevens et al., 2012), in addition to supporting high productivity at high T_a or D and lengthening the growing season over which NEE is below zero (Mueller et al., 2017; Wagle et al., 2017a).

Decoupling between NEP and E has been proposed for vegetation experiencing heat stress, when photosynthetic assimilation declines whilst transpiration is maintained for cooling of the leaf (De Kauwe et al., 2019). Reverse coupling between H and NEP implies a negative response to heat, as has been observed during heatwaves (van Gorsel et al., 2016; van Heerwaarden and Teuling, 2014). We found that reverse coupling between H and NEP (i.e., NEP was increasing when H was declining) occurred at another eight sites in the current study, with locations where E was decoupled from NEP and H (Type 2) tending to be more common in hot, minimally managed environments, and where NEP and E were both reverse coupled to H (Type 3) on colder, more highly managed farms (Fig. 2). The first and primary role of management in Australia and New Zealand was thus identified as supporting positive coupling amongst NEP, E and H and thereby managing crop stress, whether that stress originated from lack of water or abundance of heat.

5.2 Season, energy limitation and aridity

Year-round growing conditions across much of Australia and New Zealand favour a strong wintertime net carbon sink (i.e., $NEE < 0$), when low temperature limits respiration and heat stress (Campbell et al., 2014; Cleverly et al., 2013; Hutley et al., 2005; Renchon et al., 2018). For example, heavy irrigation was required in the summer for rice to obtain similar relationships amongst environmental factors as were seen in irrigated wheat during winter and springs months (Fig. 3g, i). However, wintertime cropping comes at a cost of supporting about half of the productivity as that of summer cropping, thus only three out of 19 locations in this study were evaluated during winter. Furthermore, productivity of winter pasture can be reverse-coupled to turbulent heating (e.g., AU-Otw), suggesting that some grasslands in Australia can be susceptible to heat stress, even during winter. Seasonal differences in evaporative fraction (LE/R_n) exist between irrigated wheat and maize (0.83 and 0.57, respectively; Lei and Yang, 2010), reflecting smaller potential energy limitations during wintertime than during summer. Similarly, we found that environmental factors responded

most strongly to fluctuations in R_n for maize (and rice), but that they responded to fluctuations in T_a for wheat (i.e., they had the largest α coefficient value in envPC_1).

The response of vegetation to changes in environmental factors critically depends upon whether productivity and E in a given ecosystem are energy or water limited (Donohue et al., 2009; Restrepo-Coupe et al., 2016). In energy-limited ecosystems, water is plentiful, but cloud cover restricts R_n (Hutley et al., 2005; Kanniah et al., 2013; Whitley et al., 2011). R_n and D both drive variations of E in energy-limited regions (Zhang et al., 2017), where they are strongly coherent (Peng et al., 2018). Consistent with previous observations, R_n and D were strongly and negatively coherent in this study for energy-limited regions and in areas where irrigation released water limitations, except for winter wheat, in which T_a was strongly coherent with D instead due to seasonal limitations on R_n (Fig. 3). In water-limited environments, the relationship of θ and q shifted from the woody rangeland (AU-ASM) to the grass-dominated rangeland (AU-TTE). θ is typically only related to E in water-limited environments when θ is above the wilting point (Akuraju et al., 2017), explaining the variable levels of θ coupling at AU-ASM and AU-TTE. Vegetation at AU-ASM is suspected to have an effect on surface θ via hydraulic redistribution (Cleverly et al., 2016b), thus reducing the dependence of fluxes on θ and providing an alternative explanation for the lack of correlation with θ near the surface at AU-ASM. Regardless of variations in the importance of individual environmental factors, interactions amongst all environmental factors were generally strong across our study, as has been previously inferred at AU-ASM using boundary analysis (Cleverly et al., 2013; Eamus et al., 2016).

The 19 sites in this study showed a large range of energy versus water limitations as indicated by ϕ , in which energy limitation was defined by values below unity (i.e., $R_n / [\rho_w L_v] > P$) and degree of water limitation by values above unity (i.e., $R_n / [\rho_w L_v] > P$; Fig. 4). The Canterbury Plains in New Zealand (NZ-Oxf, NZ-ADn, NZ-ADw, NZ-BFu, NZ-BFm) are generally energy limited, although a lack of precipitation during the late summer commonly pushes ϕ above unity (Graham et al., 2016), and this was when large NEP was identified for analysis in the current study (Table 2). Values of ϕ

636 near unity are likely to reflect co-limitations by energy and water (Cleverly et al., 2013; Ryu et al.,
637 2008). Currently, a general shift from energy limitations to water limitations appears to be occurring
638 in the climate system (Babst et al., 2019), making an understanding of crop responses to this transition
639 critical. By increasing θ , irrigation can tip a crop back to an energy-limited state, although irrigation
640 ultimately depends upon heavy precipitation to replenish water supplies in Australia's drylands,
641 providing only opportunistic access to irrigation in regions where irrigated agricultural production
642 might not be sustainable over the long term (Garnaut, 2008; Khan and Hanjra, 2009; Vote et al., 2015).

643 **5.3 Predictability, phenology and nonlinearities**

644 Controls on fluxes in warmer, drier climates such as those of tropical Australia can be site specific,
645 making fluxes more unpredictable and difficult to represent without local parameterisation in land
646 surface models (Haughton et al., 2018a). As a consequence, we found that predictability as inferred
647 from R^2 was low on the five northern farms in our study (AU-DaP, AU-Stp, AU-ASM, AU-TTE, AU-
648 Emr; $R^2 < 0.55$, cf. Figs. 1 and 4). Nonlinearities in regressions for these sites are consistent with the
649 presence of time-lagged perturbations to fluxes after environmental conditions have returned to normal
650 (i.e., as with pulse-response dynamics), thus acting to desynchronise environmental conditions and
651 ecosystem responses (Huxman et al., 2004). In the woody central Australian rangeland site (AU-
652 ASM), E responded exclusively to precipitation pulses, with equal sensitivity to large and small
653 fluctuations in environmental factors (Fig. 7). This variability in sensitivity to climate during
654 precipitation pulses of varying intensity thus forms the basis for variable responses of water-use
655 efficiency ($WUE = NEP/E$) observed at this location (Eamus et al., 2013). Pulse behaviour during the
656 summer of 2010/2011 was produced by heavy precipitation (Boening et al., 2012; Fasullo et al., 2013;
657 Poulter et al., 2014) in widespread, organised weather patterns which imposed cycles of strong energy
658 limitations (Cleverly et al., 2013; Cleverly et al., 2016a). Thus, similarities in the responses of
659 irrigated rice and grazed rangeland were associated with similar weather patterns during the growing

660 season at AU-ASM and AU-Cm2, despite contrasting water requirements for the rice crop at AU-Cm2
661 and for forage plants AU-ASM. Wavelet transformation of environmental factors and fluxes can
662 provide the first quantitative framework for evaluating sensitivity to precipitation pulses, for which
663 further study is merited.

664 Outside of the five northern sites (AU-DaP, AU-Stp, AU-ASM, AU-TTE, AU-Emr), R^2 followed
665 two patterns relative to aridity, depending upon management intensity. For intermediate-intensity
666 management, R^2 was small at locations where water and energy limitations were balanced ($0.8 \leq \phi \leq$
667 1.2 ; NZ-ADn, AU-Otw; $R^2 = 0.28\text{--}0.29$, cf. Figs. 1 and 4). This suggests that water limitations and
668 energy limitations can counteract one another over time, resulting in no observed net effect of
669 environmental factors on fluxes. This situation can potentially create a conundrum for land surface
670 models, where a small imbalance between compensating environmental factors can bias the output
671 (Haughton et al., 2018b). Intra-seasonal shifts in phenology, for example due to grazing or harvesting,
672 can also degrade the predictability of NEE, E and H from environmental factors. Examples of
673 phenological control of fluxes, instead of environmental control, were found at NZ-ADw, NZ-ADn
674 and NZ-BFm, all of which were exposed to 2–3 defoliation events during the analysis period. During
675 regrowth, NEE and E were constrained by low leaf area index instead of energy or water limitations.
676 To account for phenological effects, one could integrate data regarding vegetation structure (e.g., leaf
677 area index, vegetation indices), but these data would need to be measured at an equivalent frequency to
678 that of fluxes and environmental factors. Altogether for intermediate-intensity management, we found
679 three factors that reduced the innate predictability of fluxes: (i) nonlinear effects of precipitation
680 pulses; (ii) complementarity amongst coupled environmental factors in their effects on fluxes, as when
681 water and energy limitations are in temporal balance within a single season; and (iii) by undocumented
682 shifts in phenology.

683 In contrast to patterns of predictability for intermediate-intensity management, those for highly
684 intense management fell into two categories depending upon aridity: irrigation in more water-limiting

685 conditions ($\phi > 2$, AU-Lox almonds, AU-Cm1 maize and NZ-Sco dairy pasture) resulted in high flux
 686 predictability ($R^2 > 0.75$, Fig. 4), whereas moderate flux predictability ($R^2 = 0.62 \pm 0.07$) was found
 687 for sites with low values of ϕ ($\phi \leq 2$, AU-Cm1 wheat, AU-Cm2 rice, and NZ-BFm dairy farm and NZ-
 688 ADw irrigated lucerne). Even though there are environmental factors beyond the control of irrigation,
 689 irrigation practices are finely attuned to affect the environmental factors which are related to
 690 productivity, water use and heat flux, and these effects are magnified in regions where there is a large
 691 difference between on-farm and adjacent natural conditions. The most extreme example is from
 692 irrigated almonds during the final year of the Millennium Drought, where intense sensible heat
 693 advection onto the irrigated orchard from surrounding semi-arid lands pushed H to as low as -500 W
 694 m^{-2} (i.e., an input of energy into the orchard; Stevens et al., 2012). Termed "the oasis effect,"
 695 horizontal transport of energy across steep environmental gradients created by differential irrigation
 696 and evaporative cooling results in coherent variation in fluxes and scalars across the landscape (Brakke
 697 et al., 1978; Brunet et al., 1994; Cooper et al., 2003; Hanks et al., 1971). As a consequence, irrigation
 698 in Australia can lead to very high daily values of NEP in crops, both in this study (NEE *ca.* -23 g m^{-2}
 699 d^{-1} at a minimum for AU-Cm1 maize) and in previous research on rice, maize and sugarcane, which
 700 reached productivity rates of $\text{NEE} = -40 \mu\text{mol m}^{-2} \text{ s}^{-1}$ during the peak of the summer growing season
 701 (Vote et al., 2015; Webb et al., 2018).

702 This survey of environmental drivers for fluctuations in NEE, E and H leaves open a number of
 703 limitations and uncertainties which merit further investigation. These can be characterised as (i)
 704 incomplete information on carbon budgets; (ii) lack of information for relating productivity and water
 705 use to yield; and (iii) the inherent challenge of resolving reasonable relationships from nonlinear
 706 systems undergoing high levels of variability. For (i), one missing component in this study is an
 707 accounting of net biome production (NBP), which can show very different contributions to the total
 708 carbon budget from NEE. For example, a crop might be assessed as a carbon sink from NEE alone,
 709 whereas accounting for export of carbon via harvest as NBP can shift the carbon budget to a net source

(Buysse et al., 2017). Even in the absence of such a shift from carbon sink to source, failing to account for export of dissolved organic carbon from crops can result in a very large overestimation of carbon sink strength by NEE relative to NBP (Kindler et al., 2011; Webb et al., 2018). Second (ii), there are strong relationships between biomass and yield in Australian agriculture (Donohue et al., 2018), implying a close relationship between NEE (or NBP) and yield. Peak-season carbon fluxes are the most predictive for annual carbon budgets (Zscheischler et al., 2016), thus the results of our study would be particularly informative for parameterising agricultural yield models like APSIM (e.g., Donohue et al., 2018; He et al., 2014a; Luo et al., 2018; Ummenhofer et al., 2015). Third (iii), variability in precipitation is an important yet often overlooked constraint on vegetative productivity in pastures and rangelands, and this variability also affects grazing strategies in Australia (Sloat et al., 2018). Ecohydrological processes are often strongly nonlinear, amplifying intermittency and unpredictability when precipitation variability is high (Porporato et al., 2015). We found evidence for the presence of three types of nonlinearity: (a) organisation of fluxes and environmental factors around intermittent precipitation pulses; (b) over-riding control of crop phenology by mowing or grazing; and (c) compensatory effects of one or more environmental factors which ameliorated the effects of other factors. These types of nonlinearities are due to abrupt changes in biotic or environmental conditions, which are not captured well by land-surface models or analytical methods which require stationarity (e.g., auto-regression; De Keersmaecker et al., 2015). We present for the first time an analytical framework for quantifying pulse–response sensitivities on a single scale by using a wavelet–statistics conjunction approach which can incorporate information on the timing of fluctuations in addition to simple lagged averages, a necessity for land surface modelling which has recently been elucidated by Haughton et al. (2018b).

6 Conclusions

In this survey of agricultural ecosystems across Australia and New Zealand, we developed a novel statistical framework through wavelet–statistics conjunction to incorporate information on temporal

735 synchronisation between variations in turbulent fluxes (NEE, E and H) and environmental factors (R_n ,
736 q , T_a , T_s , D , G and θ). Using this approach to test hypotheses about the effects of management on
737 environment–flux relationships, we found that:

- 738 1. Coordination amongst NEE, E and H was strongly affected by management practices as
739 hypothesised. Full coupling of NEE, E and H was more frequently achieved through
740 irrigation and fertilisation practices than in minimally grazed rangelands and pastures.
741 Decoupling of NEP and E was observed at drier sites, some of which also showed reverse
742 coupling to H, illustrating the decoupling of carbon and water fluxes in response to
743 conditions conducive of heat stress (De Kauwe et al., 2019).
- 744 2. We could not fully support our second hypothesis that coordination amongst environmental
745 factors would be related to management. Large-scale differences in relationships amongst
746 environmental factors were observed across the 19 sites of this study, suggesting that
747 environmental conditions are largely site-specific and outside of management control.
748 Comparison of paired sites across management intensity categories, seasons and crop types
749 identified some environmental factors which had fixed effects across paired sites, whereas
750 dependencies with other environmental factors differed amongst sites. This suggests that a
751 subset of environmental factors are under management control at a given location, whereas
752 other environmental factors represent constraints on the agricultural system.
- 753 3. The combination of management practices which promote positive coupling of carbon and
754 water budgets (i.e., point 1) with site-specific variability of coupling amongst environmental
755 factors (i.e., point 2) generated various patterns in the predictability of fluxes from
756 environmental factors. Predictability was small in northern Australian agriculture as
757 hypothesised by Haughton et al. (2018a), with low R^2 due to nonlinear responses of fluxes
758 and environmental factors, including those due to precipitation pulses in hot climate zones.

Predictability (as a function of R^2) was also low for farms where (i) complementarity between energy and water limitations was apparent ($0.8 \leq \phi \leq 1.2$) and (ii) management activities such as grazing or harvesting induced a phenological response and release from environmental constraints. Conversely, irrigation in water-limited environments resulted in very high predictability of variations in fluxes from knowledge of environmental factors.

By incorporating timing and temporal variability into a statistical framework, wavelet–regression conjunction modelling has the capability of transforming our understanding of how ecosystems respond to fluctuations in climate, to the occurrence of nonstationarities such as precipitation pulses and extreme weather events, and to climate change by helping to analytically separate the effects of fluctuations, nonstationarities and trends. Several potential applications arise from this work, including analysis of longer-term phenological trends characterised by satellite imagery, development of a better understanding of drought impacts on crops, comparison of crops with differing physiognomy, and analysis of greenup/brown-down dynamics.

Acknowledgments

The study used data from Terrestrial Ecosystem Research Network (TERN, <http://tern.org.au>), supported by the Australian Government through the National Collaborative Research Infrastructure Strategy (NCRIS). The authors would like to further acknowledge funding through the Australian Research Council (ARC) and the National Water Commission through Programs 3 (surface water–groundwater interactions, AU-TTE) and 4 (groundwater–vegetation–atmosphere interactions, AU-Gat) of the National Centre for Groundwater Research and Training (a part of the NCRIS Groundwater project). Further funding for AU-Gat was provided by ARC and the Victoria Department of Economic Development, Jobs, Transport and Resources (ARC LP140100871). NZ funding sources included Landcare Research and NZ government. We would also like to thank Eva van Gorsel for her insights

and discussion during early planning stages of this study, and two anonymous reviewers whose suggestions have helped to improve manuscript quality.

7 REFERENCES

- Abry, P. and Didier, G., 2018. Wavelet eigenvalue regression for n-variate operator fractional Brownian motion. *J. Multivar. Anal.* 168: 75-104, DOI: 10.1016/j.jmva.2018.06.007.
- Adamson, D., Loch, A. and Schwabe, K., 2017. Adaptation responses to increasing drought frequency. *Aust. J. Agr. Resour. Econ.* 61: 385-403, DOI: 10.1111/1467-8489.12214.
- Akuraju, V.R., Ryu, D., George, B., Ryu, Y. and Dassanayake, K., 2017. Seasonal and inter-annual variability of soil moisture stress function in dryland wheat field, Australia. *Agric. For. Meteorol.* 232: 489-499, DOI: 10.1016/j.agrformet.2016.10.007.
- Australian Bureau of Statistics, 2018. *Agricultural Commodities*, Australia, 2016–2017, Commonwealth of Australia, Canberra.
- Babst, F., Bouriaud, O., Poulter, B., Trouet, V., Girardin, M.P. and Frank, D.C., 2019. Twentieth century redistribution in climatic drivers of global tree growth. *Sci. Adv.* 5: eaat4313, DOI: 10.1126/sciadv.aat4313.
- Behtari, B., Jafarian, Z. and Alikhani, H., 2019. Temperature sensitivity of soil organic matter decomposition in response to land management in semi-arid rangelands of Iran. *Catena*. 179: 210-219, DOI: 10.1016/j.catena.2019.03.043.
- Beringer, J., Hutley, L.B., Abramson, D., Arndt, S.K., Briggs, P., Bristow, M., Canadell, J.G., Cernusak, L.A., Eamus, D., Edwards, A.C., Evans, B.J., Fest, B., Goergen, K., Grover, S.P., Hacker, J., Haverd, V., Kanniah, K., Livesley, S.J., Lynch, A., Maier, S., Moore, C., Raupach, M., Russell-Smith, J., Scheiter, S., Tapper, N.J. and Uotila, P., 2015. Fire in Australian savannas: from leaf to landscape. *Glob. Change Biol.* 21: 62-81, DOI: 10.1111/gcb.12686.
- Beringer, J., Hutley, L.B., Hacker, J.M., Neininger, B. and U, K.T.P., 2011. Patterns and processes of carbon, water and energy cycles across northern Australian landscapes: From point to region. *Agric. For. Meteorol.* 151: 1409-1416, DOI: 10.1016/j.agrformet.2011.05.003.
- Beringer, J., Hutley, L.B., McHugh, I., Arndt, S.K., Campbell, D., Cleugh, H.A., Cleverly, J., Resco de Dios, V., Eamus, D., Evans, B., Ewenz, C., Grace, P., Griebel, A., Haverd, V., Hinko-Najera, N., Huete, A., Isaac, P., Kanniah, K., Leuning, R., Liddell, M.J., Macfarlane, C., Meyer, W., Moore, C., Pendall, E., Phillips, A., Phillips, R.L., Prober, S.M., Restrepo-Coupe, N., Rutledge, S., Schroder, I., Silberstein, R., Southall, P., Yee, M.S., Tapper, N.J., van Gorsel, E., Voté, C., Walker, J. and Wardlaw, T., 2016. An introduction to the Australian and New Zealand flux tower network – OzFlux. *Biogeosciences*. 13: 5895-5916, DOI: 10.5194/bg-13-5895-2016.
- Beringer, J., McHugh, I., Hutley, L.B., Isaac, P. and Kljun, N., 2017. Technical note: Dynamic INtegrated Gap-filling and partitioning for OzFlux (DINGO). *Biogeosciences*. 14: 1457-1460, DOI: 10.5194/bg-14-1457-2017.
- Berko, H., Etheridge, D., Loh, D., Kuske, T., Colin, A., Gregory, R., Spencer, D., Law, R., Zegelin, S. and Feitz, A., 2012. Installation Report for Arcturus (ARA): An inland baseline station for the continuous measurement of atmospheric greenhouse gases. 1922103616, Geoscience Australia, Canberra.

Best, M.J., Abramowitz, G., Johnson, H.R., Pitman, A.J., Balsamo, G., Boone, A., Cuntz, M.,
Decharme, B., Dirmeyer, P.A., Dong, J., Ek, M., Guo, Z., Haverd, V., Van den Hurk, B.J.J.,
Nearing, G.S., Pak, B., Peters-Lidard, C., Santanello, J.A., Jr., Stevens, L. and Vuichard, N.,
2015. The Plumbing of Land Surface Models: Benchmarking Model Performance. *J.*
Hydrometeor. 16: 1425-1442, DOI: 10.1175/JHM-D-14-0158.1.

Boening, C., Willis, J.K., Landerer, F.W., Nerem, R.S. and Fasullo, J., 2012. The 2011 La Niña: So
strong, the oceans fell. *Geophys. Res. Lett.* 39: L19602, DOI: 10.1029/2012gl053055.

Brakke, T.W., Verma, S.B. and Rosenberg, N.J., 1978. Local and regional components of sensible heat
advection. *J. Appl. Meteor.* 17: 935-963.

Brown, M., Whitehead, D., Hunt, J.E., Clough, T.J., Arnold, G.C., Baisden, W.T. and Sherlock, R.R.,
2009. Regulation of soil surface respiration in a grazed pasture in New Zealand. *Agric. For.*
Meteor. 149: 205-213, DOI: 10.1016/j.agrformet.2008.08.005.

Brunet, Y., Itier, B., McAneney, J. and Lagouarde, J.P., 1994. Downwind evolution of scalar fluxes
and surface resistance under conditions of local advection. Part II: Measurements over barley.
Agric. For. Meteor. 71: 227-245.

Budyko, M.I., 1974. *Climate and Life*. Academic Press, San Diego, CA, 508 pp.

Buyse, P., Bodson, B., Debacq, A., De Ligne, A., Heinesch, B., Manise, T., Moureaux, C. and
Aubinet, M., 2017. Carbon budget measurement over 12 years at a crop production site in the
silty-loam region in Belgium. *Agric. For. Meteor.* 246: 241-255, DOI:
10.1016/j.agrformet.2017.07.004.

Cai, Q., Zhang, Y.L., Sun, Z.X., Zheng, J.M., Bai, W., Zhang, Y., Liu, Y., Feng, L.S., Feng, C.,
Zhang, Z., Yang, N., Evers, J.B. and Zhang, L.Z., 2017. Morphological plasticity of root
growth under mild water stress increases water use efficiency without reducing yield in maize.
Biogeosciences. 14: 3851-3858.

Cammarano, D. and Tian, D., 2018. The effects of projected climate and climate extremes on a winter
and summer crop in the southeast USA. *Agric. For. Meteor.* 248: 109-118, DOI:
10.1016/j.agrformet.2017.09.007.

Campbell, D.I., Smith, J., Goodrich, J.P., Wall, A.M. and Schipper, L.A., 2014. Year-round growing
conditions explains large CO₂ sink strength in a New Zealand raised peat bog. *Agric. For.*
Meteor. 192: 59-68, DOI: 10.1016/j.agrformet.2014.03.003.

Chen, X., Su, Z., Ma, Y., Cleverly, J. and Liddell, M., 2017. An accurate estimate of monthly mean
land surface temperatures from MODIS clearsky retrievals. *J. Hydrometeor.* 18: 2827-2847,
DOI: 10.1175/jhm-d-17-0009.1.

Chi, J., Waldo, S., Pressley, S., O'Keeffe, P., Huggins, D., Stöckle, C., Pan, W.L., Brooks, E. and
Lamb, B., 2016. Assessing carbon and water dynamics of no-till and conventional tillage
cropping systems in the inland Pacific Northwest US using the eddy covariance method. *Agric.*
For. Meteor. 218-219: 37-49, DOI: 10.1016/j.agrformet.2015.11.019.

Cleverly, J., 2019. Agricultural ecosystems collection. TERN OzFlux: Australian and New Zealand
Flux Research and Monitoring Network, hdl.handle.net/102.100.100/79013.

Cleverly, J., Boulain, N., Villalobos-Vega, R., Grant, N., Faux, R., Wood, C., Cook, P.G., Yu, Q.,
Leigh, A. and Eamus, D., 2013. Dynamics of component carbon fluxes in a semi-arid *Acacia*
woodland, central Australia. *J. Geophys. Res.: Biogeosci.* 118: 1168-1185, DOI:
10.1002/jgrg.20101.

865 Cleverly, J., Eamus, D., Edwards, W., Grant, M., Grundy, M.J., Held, A., Karan, M., Lowe, A.J.,
866 Prober, S.M., Sparrow, B. and Morris, B., 2019. TERN, Australia's Land Observatory:
867 addressing the global challenge of forecasting ecosystem responses to climate variability and
868 change. *Environ. Res. Lett.* 14: 095004, DOI: 10.1088/1748-9326/ab33cb.

869 Cleverly, J., Eamus, D., Luo, Q., Restrepo Coupe, N., Kljun, N., Ma, X., Ewenz, C., Li, L., Yu, Q. and
870 Huete, A., 2016a. The importance of interacting climate modes on Australia's contribution to
871 global carbon cycle extremes. *Sci. Rep.* 6: 23113, DOI: 10.1038/srep23113.

872 Cleverly, J., Eamus, D., Restrepo Coupe, N., Chen, C., Maes, W., Li, L., Faux, R., Santini, N.S.,
873 Rumman, R., Yu, Q. and Huete, A., 2016b. Soil moisture controls on phenology and
874 productivity in a semi-arid critical zone. *Sci. Total Environ.* 568: 1227-1237, DOI:
875 10.1016/j.scitotenv.2016.05.142.

876 Cleverly, J., Eamus, D., Van Gorsel, E., Chen, C., Rumman, R., Luo, Q., Restrepo Coupe, N., Li, L.,
877 Kljun, N., Faux, R., Yu, Q. and Huete, A., 2016c. Productivity and evapotranspiration of two
878 contrasting semiarid ecosystems following the 2011 global carbon land sink anomaly. *Agric.*
879 *For. Meteor.* 220: 151-159, DOI: 10.1016/j.agrformet.2016.01.086.

880 Cleverly, J., Thibault, J.R., Teet, S.B., Tashjian, P., Hipps, L.E., Dahm, C.N. and Eamus, D., 2015.
881 Flooding regime impacts on radiation, evapotranspiration and latent heat fluxes over
882 groundwater-dependent riparian cottonwood and saltcedar forests. *Adv. Meteorol.* 2015:
883 935060, DOI: 10.1155/2015/935060.

884 Collineau, S. and Brunet, Y., 1993. Detection of turbulent coherent motions in a forest canopy part I:
885 Wavelet analysis. *Bound.-Lay. Meteor.* 65: 357-379, DOI: 10.1007/bf00707033.

886 Cooper, D., Eichinger, W., Archuleta, J., Hipps, L., Kao, J., Leclerc, M., Neale, C. and Prueger, J.,
887 2003. Spatial source-area analysis of three-dimensional moisture fields from LIDAR, eddy
888 covariance, and a footprint model. *Agric. For. Meteor.* 114: 213-234.

889 Cunningham, S.C., Mac Nally, R., Baker, P.J., Cavagnaro, T.R., Beringer, J., Thomson, J.R. and
890 Thompson, R.M., 2015. Balancing the environmental benefits of reforestation in agricultural
891 regions. *Perspect. Plant Ecol. Evol. Syst.* 17: 301-317, DOI: 10.1016/j.ppees.2015.06.001.

892 Cuxart, J., Morales, G., Terradellas, E. and Yague, C., 2002. Study of coherent structures and
893 estimation of the pressure transport terms for the nocturnal stable boundary layer. *Bound.-Lay.*
894 *Meteor.* 105: 305-328, DOI: 10.1023/a:1019974021434.

895 Davis, P.A., Brown, J.C., Saunders, M., Lanigan, G., Wright, E., Fortune, T., Burke, J., Connolly, J.,
896 Jones, M.B. and Osborne, B., 2010. Assessing the effects of agricultural management practices
897 on carbon fluxes: Spatial variation and the need for replicated estimates of Net Ecosystem
898 Exchange. *Agric. For. Meteor.*

899 De Kauwe, M.G., Medlyn, B.E., Pitman, A.J., Drake, J.E., Ukkola, A., Griebel, A., Pendall, E., Prober,
900 S. and Roderick, M., 2019. Examining the evidence for decoupling between photosynthesis and
901 transpiration during heat extremes. *Biogeosciences.* 16: 903-916, DOI: 10.5194/bg-16-903-
902 2019.

903 De Keersmaecker, W., Lhermitte, S., Tits, L., Honnay, O., Somers, B. and Coppin, P., 2015. A model
904 quantifying global vegetation resistance and resilience to short-term climate anomalies and
905 their relationship with vegetation cover. *Glob. Ecol. Biogeogr.* 24: 539-548, DOI:
906 10.1111/geb.12279.

907 Donohue, R.J., Lawes, R.A., Mata, G., Gobbett, D. and Ouzman, J., 2018. Towards a national, remote-
908 sensing-based model for predicting field-scale crop yield. *Field Crop. Res.* 227: 79-90, DOI:
909 10.1016/j.fcr.2018.08.005.

910 Donohue, R.J., McVicar, T.R. and Roderick, M.L., 2009. Climate-related trends in Australian
911 vegetation cover as inferred from satellite observations, 1981-2006. *Glob. Change Biol.* 15:
912 1025-1039.

913 Dreccer, M.F., Fainges, J., Whish, J., Ogbonnaya, F.C. and Sadras, V.O., 2018. Comparison of
914 sensitive stages of wheat, barley, canola, chickpea and field pea to temperature and water stress
915 across Australia. *Agric. For. Meteor.* 248: 275-294.

916 Dresel, P.E., Dean, J.F., Perveen, F., Webb, J.A., Hekmeijer, P., Adelana, S.M. and Daly, E., 2018.
917 Effect of Eucalyptus plantations, geology, and precipitation variability on water resources in
918 upland intermittent catchments. *J. Hydrol.* 564: 723-739, DOI: 10.1016/j.jhydrol.2018.07.019.

919 Drewniak, B.A., Mishra, U., Song, J., Prell, J. and Kotamarthi, V.R., 2015. Modeling the impact of
920 agricultural land use and management on US carbon budgets. *Biogeosciences*. 12: 2119-2129.

921 Eamus, D., Cleverly, J., Boulain, N., Grant, N., Faux, R. and Villalobos-Vega, R., 2013. Carbon and
922 water fluxes in an arid-zone *Acacia* savanna woodland: An analyses of seasonal patterns and
923 responses to rainfall events. *Agric. For. Meteor.* 182–183: 225–238, DOI:
924 10.1016/j.agrformet.2013.04.020.

925 Eamus, D., Huete, A., Cleverly, J., Nolan, R.H., Ma, X., Tarin, T. and Santini, N.S., 2016. Mulga, a
926 major tropical dry open forest of Australia: recent insights to carbon and water fluxes. *Environ.*
927 *Res. Lett.* 11: 125011, DOI: 10.1088/1748-9326/11/12/125011.

928 Ellis, N.R. and Albrecht, G.A., 2017. Climate change threats to family farmers' sense of place and
929 mental wellbeing: A case study from the Western Australian Wheatbelt. *Soc. Sci. Med.* 175:
930 161-168, DOI: 10.1016/j.socscimed.2017.01.009.

931 Etheridge, D., Luhr, A., Loh, Z., Leuning, R., Spencer, D., Steele, P., Zegelin, S., Allison, C.,
932 Krummel, P., Leist, M. and van der Schoot, M., 2011. Atmospheric monitoring of the
933 CO₂CRC Otway Project and lessons for large scale CO₂ storage projects. *Energy Procedia*. 4:
934 3666-3675, DOI: 10.1016/j.egypro.2011.02.298.

935 Fasullo, J.T., Boening, C., Landerer, F.W. and Nerem, R.S., 2013. Australia's unique influence on
936 global sea level in 2010-2011. *Geophys. Res. Lett.* 40: 4368-4373, DOI: 10.1002/grl.50834.

937 Foley, J.A., DeFries, R., Asner, G.P., Barford, C., Bonan, G., Carpenter, S.R., Chapin, F.S., Coe, M.T.,
938 Daily, G.C., Gibbs, H.K., Helkowski, J.H., Holloway, T., Howard, E.A., Kucharik, C.J.,
939 Monfreda, C., Patz, J.A., Prentice, I.C., Ramankutty, N. and Snyder, P.K., 2005. Global
940 consequences of land use. *Science*. 309: 570-574, DOI: 10.1126/science.1111772.

941 Garnaut, R., 2008. The Garnaut climate change review : final report / Ross Garnaut. Cambridge
942 University Press, Port Melbourne, Vic. .:

943 Graham, S.L., Kochendorfer, J., McMillan, A.M.S., Duncan, M.J., Srinivasan, M.S. and Hertzog, G.,
944 2016. Effects of agricultural management on measurements, prediction, and partitioning of
945 evapotranspiration in irrigated grasslands. *Agric. Water Manage.* 177: 340-347, DOI:
946 10.1016/j.agwat.2016.08.015.

947 Grinsted, A., Moore, J.C. and Jevrejeva, S., 2004. Application of the cross wavelet transform and
948 wavelet coherence to geophysical time series. *Nonlinear Process Geophys.* 11: 561-566.

949 Guan, H., He, X. and Zhang, X., 2015. A comprehensive examination of global atmospheric CO₂
950 teleconnections using wavelet-based multi-resolution analysis. *Environmental Earth Sciences*.
951 74: 7239-7253, DOI: 10.1007/s12665-015-4705-z.

952 Hanks, R.J., Allen, L.H., Jr. and Gardner, H.B., 1971. Advection and evapotranspiration of wide-row
953 sorghum in the Central Great Plains. *Agron. J.* 63: 520-527.

954 Hao, X.M., Zhang, S.H., Li, W.H., Duan, W.L., Fang, G.H., Zhang, Y. and Guo, B., 2018. The
955 uncertainty of Penman-Monteith method and the energy balance closure problem. *J. Geophys.*
956 *Res.: Atmos.* 123: 7433-7443, DOI: 10.1029/2018jd028371.

957 Hargrove, W.W. and Pickering, J., 1992. Pseudoreplication: a *sine qua non* for regional ecology.
958 *Landsc. Ecol.* 6: 251-258, DOI: 10.1007/bf00129703.

959 Haughton, N., Abramowitz, G., De Kauwe, M.G. and Pitman, A.J., 2018a. Does predictability of
960 fluxes vary between FLUXNET sites? *Biogeosciences.* 15: 4495-4513, DOI: 10.5194/bg-15-
961 4495-2018.

962 Haughton, N., Abramowitz, G. and Pitman, A.J., 2018b. On the predictability of land surface fluxes
963 from meteorological variables. *Geosci. Model Dev.* 11: 195-212, DOI: 10.5194/gmd-11-195-
964 2018.

965 He, L., Cleverly, J., Chen, C., Yang, X., Li, J., Liu, W. and Yu, Q., 2014a. Diverse responses of winter
966 wheat yield and water use to climate change and variability on the semiarid Loess Plateau in
967 China. *Agron. J.* 106: 1169–1178, DOI: 10.2134/agronj13.0321.

968 He, L., Cleverly, J., Wang, B., Jin, N., Mi, C., Liu, D.L. and Yu, Q., 2018. Multi-model ensemble
969 projections of future extreme heat stress on rice across southern China. *Theor. Appl. Climatol.*
970 133: 1107-1118, DOI: 10.1007/s00704-017-2240-4.

971 He, X. and Guan, H., 2013. Multiresolution analysis of precipitation teleconnections with large-scale
972 climate signals: A case study in South Australia. *Water Resour. Res.* 49: 6995-7008, DOI:
973 10.1002/wrcr.20560.

974 He, X., Guan, H., Zhang, X. and Simmons, C.T., 2014b. A wavelet-based multiple linear regression
975 model for forecasting monthly rainfall. *Int. J. Climatol.* 34: 1898–1912, DOI:
976 10.1002/joc.3809.

977 Hsu, K.-I., Gupta, H.V., Gao, X., Sorooshian, S. and Imam, B., 2002. Self-organizing linear output
978 map (SOLO): An artificial neural network suitable for hydrologic modeling and analysis.
979 *Water Resour. Res.* 38: 1302, DOI: 10.1029/2001wr000795.

980 Hunt, J.E., Laubach, J., Barthel, M., Fraser, A. and Phillips, R.L., 2016. Carbon budgets for an
981 irrigated intensively grazed dairy pasture and an unirrigated winter-grazed pasture.
982 *Biogeosciences.* 13: 2927-2944, DOI: 10.5194/bg-13-2927-2016.

983 Hutley, L.B., Beringer, J., Isaac, P.R., Hacker, J.M. and Cernusak, L.A., 2011. A sub-continental scale
984 living laboratory: Spatial patterns of savanna vegetation over a rainfall gradient in northern
985 Australia. *Agric. For. Meteorol.* 151: 1417–1428, DOI: 10.1016/j.agrformet.2011.03.002.

986 Hutley, L.B., Leuning, R., Beringer, J. and Cleugh, H.A., 2005. The utility of the eddy covariance
987 techniques as a tool in carbon accounting: tropical savanna as a case study. *Aust. J. Bot.* 53:
988 663–675, DOI: 10.1071/BT04147.

989 Huxman, T.E., Snyder, K.A., Tissue, D., Leffler, A.J., Ogle, K., Pockman, W.T., Sandquist, D.R.,
990 Potts, D.L. and Schwinning, S., 2004. Precipitation pulses and carbon fluxes in semiarid and
991 arid ecosystems. *Oecologia.* 141: 254–268, DOI: 10.1007/s00442-004-1682-4.

992 Isaac, P., Cleverly, J., McHugh, I., van Gorsel, E., Ewenz, C. and Beringer, J., 2017. OzFlux data:
993 network integration from collection to curation. *Biogeosciences.* 14: 2903-2928, DOI:
994 10.5194/bg-14-2903-2017.

995 Jeong, S.-J., Ho, C.-H., Piao, S., Kim, J., Ciais, P., Lee, Y.-B., Jhun, J.-G. and Park, S.K., 2014.
996 Effects of double cropping on summer climate of the North China Plain and neighbouring
997 regions. *Nat. Clim. Change.* 4: 615, DOI: 10.1038/nclimate2266.

998 Jin, Z., Zhuang, Q.L., Wang, J.L., Archontoulis, S.V., Zobel, Z. and Kotamarthi, V.R., 2017. The
999 combined and separate impacts of climate extremes on the current and future US rainfed maize
000 and soybean production under elevated CO₂. *Glob. Change Biol.* 23: 2687-2704, DOI:
001 10.1111/gcb.13617.

002 Kanniah, K.D., Beringer, J. and Hutley, L., 2013. Exploring the link between clouds, radiation, and
003 canopy productivity of tropical savannas. *Agric. For. Meteor.* 182–183: 304-313, DOI:
004 10.1016/j.agrformet.2013.06.010.

005 Katul, G.G. and Parlange, M.B., 1995. The spatial structure of turbulence at production wave-numbers
006 using orthonormal wavelets. *Bound.-Lay. Meteor.* 75: 81-108, DOI: 10.1007/bf00721045.

007 Khan, S. and Hanjra, M.A., 2009. Footprints of water and energy inputs in food production - Global
008 perspectives. *Food Policy*. 34: 130-140.

009 Kindler, R., Siemens, J., Kaiser, K., Walmsley, D.C., Bernhofer, C., Buchmann, N., Cellier, P.,
010 Eugster, W., Gleixner, G., Grunwald, T., Heim, A., Ibrom, A., Jones, S.K., Jones, M., Klumpp,
011 K., Kutsch, W., Larsen, K.S., Lehuger, S., Loubet, B., McKenzie, R., Moors, E., Osborne, B.,
012 Pilegaard, K., Rebmann, C., Saunders, M., Schmidt, M.W.I., Schrumpf, M., Seyfferth, J.,
013 Skiba, U., Soussana, J.F., Sutton, M.A., Tefs, C., Vowinckel, B., Zeeman, M.J. and
014 Kaupenjohann, M., 2011. Dissolved carbon leaching from soil is a crucial component of the net
015 ecosystem carbon balance. *Glob. Change Biol.* 17: 1167-1185, DOI: 10.1111/j.1365-
016 2486.2010.02282.x.

017 Kirschbaum, M.U.F., Schipper, L.A., Mudge, P.L., Rutledge, S., Puche, N.J.B. and Campbell, D.I.,
018 2017. The trade-offs between milk production and soil organic carbon storage in dairy systems
019 under different management and environmental factors. *Sci. Total Environ.* 577: 61-72, DOI:
020 10.1016/j.scitotenv.2016.10.055.

021 Lara, M.J., Johnson, D.R., Andresen, C., Hollister, R.D. and Tweedie, C.E., 2017. Peak season carbon
022 exchange shifts from a sink to a source following 50+years of herbivore exclusion in an Arctic
023 tundra ecosystem. *J. Ecol.* 105: 122-131, DOI: 10.1111/1365-2745.12654.

024 Laubach, J. and Hunt, J.E., 2018. Greenhouse-gas budgets for irrigated dairy pasture and a winter-
025 forage kale crop. *Agric. For. Meteor.* 258: 117-134, DOI: 10.1016/j.agrformet.2017.04.013.

026 Laubach, J., Hunt, J.E., Graham, S.L., Buxton, R.P., Rogers, G.N.D., Mudge, P.L., Carrick, S. and
027 Whitehead, D., 2019. Irrigation increases forage production of newly established lucerne but
028 enhances net ecosystem carbon losses. *Sci. Total Environ.* 689: 921-936, DOI:
029 10.1016/j.scitotenv.2019.06.407.

030 Lei, H. and Yang, D., 2010. Interannual and seasonal variability in evapotranspiration and energy
031 partitioning over an irrigated cropland in the North China Plain. *Agric. For. Meteor.* 150: 581-
032 589.

033 Loh, Z., Leuning, R., Zegelin, S., Etheridge, D., Bai, M., Naylor, T. and Griffith, D., 2009. Testing
034 Lagrangian atmospheric dispersion modelling to monitor CO₂ and CH₄ leakage from
035 geosequestration. *Atmos. Environ.* 43: 2602-2611, DOI: 10.1016/j.atmosenv.2009.01.053.

036 Luo, Q., O’Leary, G., Cleverly, J. and Eamus, D., 2018. Effectiveness of time of sowing and cultivar
037 choice for managing climate change: wheat crop phenology and water use efficiency. *Int. J.*
038 *Biometeor.* 62: 1049-1061, DOI: 10.1007/s00484-018-1508-4.

039 Lynch, A.H., Abramson, D., Görden, K., Beringer, J. and Uotila, P., 2007. Influence of savanna fire on
040 Australian monsoon season precipitation and circulation as simulated using a distributed
041 computing environment. *Geophys. Res. Lett.* 34: L20801, DOI: 10.1029/2007GL030879.

042 Ma, X., Huete, A., Cleverly, J., Eamus, D., Chevallier, F., Joiner, J., Poulter, B., Zhang, Y., Guanter,
043 L., Meyer, W., Xie, Z. and Ponce-Campos, G., 2016. Drought rapidly diminishes the large net
044 CO₂ uptake in 2011 over semi-arid Australia. *Sci. Rep.* 6: 37747, DOI: 10.1038/srep37747.

045 Mallawaarachchi, T., Nauges, C., Sanders, O. and Quiggin, J., 2017. State-contingent analysis of
046 farmers' response to weather variability: irrigated dairy farming in the Murray Valley,
047 Australia. *Aust. J. Agr. Resour. Econ.* 61: 36-55, DOI: 10.1111/1467-8489.12193.

048 Meier, E.A., Thorburn, P.J., Kragt, M.E., Dumbrell, N.P., Biggs, J.S., Hoyle, F.C. and van Rees, H.,
049 2017. Greenhouse gas abatement on southern Australian grains farms: Biophysical potential
050 and financial impacts. *Agric. Syst.* 155: 147-157, DOI: 10.1016/j.agsy.2017.04.012.

051 Moffat, A.M., Papale, D., Reichstein, M., Hollinger, D.Y., Richardson, A.D., Barr, A.G., Beckstein,
052 C., Braswell, B.H., Churkina, G., Desai, A.R., Falge, E., Gove, J.H., Heimann, M., Hui, D.F.,
053 Jarvis, A.J., Kattge, J., Noormets, A. and Stauch, V.J., 2007. Comprehensive comparison of
054 gap-filling techniques for eddy covariance net carbon fluxes. *Agric. For. Meteorol.* 147: 209-232.

055 Moinet, Y.G., Midwood, J.A., Hunt, E.J., Rumpel, C., Millard, P. and Chabbi, A., 2019. Grassland
056 Management Influences the Response of Soil Respiration to Drought. *Agronomy*. 9, DOI:
057 10.3390/agronomy9030124.

058 Mudge, P.L., Wallace, D.F., Rutledge, S., Campbell, D.I., Schipper, L.A. and Hosking, C.L., 2011.
059 Carbon balance of an intensively grazed temperate pasture in two climatically contrasting
060 years. *Agric. Ecosyst. Environ.* 144: 271-280, DOI: 10.1016/j.agee.2011.09.003.

061 Mueller, N.D., Rhines, A., Butler, E.E., Ray, D.K., Siebert, S., Holbrook, N.M. and Huybers, P., 2017.
062 Global relationships between cropland intensification and summer temperature extremes over
063 the last 50 years. *J. Clim.* 30: 7505-7528, DOI: 10.1175/jcli-d-17-0096.1.

064 Murphy, B.P., Paron, P., Prior, L.D., Boggs, G.S., Franklin, D.C. and Bowman, D., 2010. Using
065 generalized autoregressive error models to understand fire-vegetation-soil feedbacks in a
066 mulga-spinifex landscape mosaic. *J. Biogeogr.* 37: 2169-2182, DOI: 10.1111/j.1365-
067 2699.2010.02359.x.

068 Orgill, S.E., Waters, C.M., Melville, G., Toole, I., Alemseged, Y. and Smith, W., 2017. Sensitivity of
069 soil organic carbon to grazing management in the semi-arid rangelands of south-eastern
070 Australia. *Rangeland J.* 39: 153-167, DOI: 10.1071/rj16020.

071 Peng, L., Li, D. and Sheffield, J., 2018. Drivers of variability in atmospheric evaporative demand:
072 multiscale spectral analysis based on observations and physically based modeling. *Water*
073 *Resour. Res.* 54: 3510-3529, DOI: 10.1029/2017WR022104.

074 Percival, D.B. and Walden, A.T., 2000. Wavelet Methods for Time Series Analysis. Cambridge Series
075 in Statistical and Probabilistic Mathematics. Cambridge University Press, New York, NY.

076 Porporato, A., Feng, X., Manzoni, S., Mau, Y., Parolari, A.J. and Vico, G., 2015. Ecohydrological
077 modeling in agroecosystems: Examples and challenges. *Water Resour. Res.* 51: 5081-5099,
078 DOI: 10.1002/2015WR017289.

079 Poulter, B., Frank, D., Ciais, P., Myneni, R.B., Andela, N., Bi, J., Broquet, G., Canadell, J.G.,
080 Chevallier, F., Liu, Y.Y., Running, S.W., Sitch, S. and van der Werf, G.R., 2014. Contribution
081 of semi-arid ecosystems to interannual variability of the global carbon cycle. *Nature*. 509: 600–
082 603, DOI: 10.1038/nature13376.

083 Rashid, M.A., Andersen, M.N., Wollenweber, B., Zhang, X.Y. and Olesen, J.E., 2018. Acclimation to
084 higher VPD and temperature minimized negative effects on assimilation and grain yield of
085 wheat. *Agric. For. Meteorol.* 248: 119-129, DOI: 10.1016/j.agrformet.2017.09.018.

086 Ratcliffe, J.L., Campbell, D.I., Clarkson, B.R., Wall, A.M. and Schipper, L.A., 2019. Water table
087 fluctuations control CO₂ exchange in wet and dry bogs through different mechanisms. *Sci.*
088 *Total Environ.* 655: 1037-1046, DOI: 10.1016/j.scitotenv.2018.11.151.

089 Raupach, M.R., Haverd, V. and Briggs, P.R., 2013. Sensitivities of the Australian terrestrial water and
090 carbon balances to climate change and variability. *Agric. For. Meteorol.* 182–183: 277-291, DOI:
091 10.1016/j.agrformet.2013.06.017.

092 Regan, C.M., Connor, J.D., Segaran, R.R., Meyer, W.S., Bryan, B.A. and Ostendorf, B., 2017. Climate
093 change and the economics of biomass energy feedstocks in semi-arid agricultural landscapes:
094 A spatially explicit real options analysis. *J. Environ. Manage.* 192: 171-183, DOI:
095 10.1016/j.jenvman.2017.01.049.

096 Renchon, A.A., Griebel, A., Metzen, D., Williams, C.A., Medlyn, B., Duursma, R.A., Barton, C.V.M.,
097 Maier, C., Boer, M.M., Isaac, P., Tissue, D., Resco de Dios, V. and Pendall, E., 2018. Upside-
098 down fluxes Down Under: CO₂ net sink in winter and net source in summer in a temperate
099 evergreen broadleaf forest. *Biogeosciences*. 15: 3703-3716, DOI: 10.5194/bg-15-3703-2018.

100 Restrepo-Coupe, N., Huete, A., Davies, K., Cleverly, J., Beringer, J., Eamus, D., van Gorsel, E.,
101 Hutley, L.B. and Meyer, W.S., 2016. MODIS vegetation products as proxies of photosynthetic
102 potential along a gradient of meteorologically and biologically driven ecosystem productivity.
103 *Biogeosciences*. 13: 5587-5608, DOI: 10.5194/bg-13-5587-2016.

104 Rhif, M., Abbes, A.B., Farah, I.R., Martínez, B. and Sang, Y., 2019. Wavelet transform application
105 for/in non-stationary time-series analysis: A review. *Appl. Sci.* 9, DOI: 10.3390/app9071345.

106 Rutledge, S., Mudge, P.L., Campbell, D.I., Woodward, S.L., Goodrich, J.P., Wall, A.M., Kirschbaum,
107 M.U.F. and Schipper, L.A., 2015. Carbon balance of an intensively grazed temperate dairy
108 pasture over four years. *Agric. Ecosyst. Environ.* 206: 10-20, DOI:
109 10.1016/j.agee.2015.03.011.

110 Ryu, Y., Baldocchi, D.D., Ma, S. and Hehn, T., 2008. Interannual variability of evapotranspiration and
111 energy exchange over an annual grassland in California. *J. Geophys. Res.: Atmos.* 113:
112 D09104.

113 Schaller, C., Göckede, M. and Foken, T., 2017. Flux calculation of short turbulent events –
114 comparison of three methods. *Atmos. Meas. Tech.* 10: 869-880, DOI: 10.5194/amt-10-869-
115 2017.

116 Schipper, L.A., Petrie, O.J., O'Neill, T.A., Mudge, P.L., Liáng, L.L., Robinson, J.M. and Arcus, V.L.,
117 2019. Shifts in temperature response of soil respiration between adjacent irrigated and non-
118 irrigated grazed pastures. *Agric. Ecosyst. Environ.* 285: 106620, DOI:
119 10.1016/j.agee.2019.106620.

120 Shao, C.L., Chen, J.Q., Li, L.H., Dong, G., Han, J.J., Abraha, M. and John, R., 2017. Grazing effects
121 on surface energy fluxes in a desert steppe on the Mongolian Plateau. *Ecol. Appl.* 27: 485-502,
122 DOI: 10.1002/eap.1459.

123 Shi, H., Li, L., Eamus, D., Cleverly, J., Huete, A., Beringer, J., Yu, Q., van Gorsel, E. and Hutley, L.,
124 2014. Intrinsic climate dependency of ecosystem light and water-use-efficiencies across
125 Australian biomes. *Environ. Res. Lett.* 9: 104002, DOI: 10.1088/1748-9326/9/10/104002.

126 Sloat, L.L., Gerber, J.S., Samberg, L.H., Smith, W.K., Herrero, M., Ferreira, L.G., Godde, C.M. and
127 West, P.C., 2018. Increasing importance of precipitation variability on global livestock grazing
128 lands. *Nat. Clim. Change*. 8: 214-218, DOI: 10.1038/s41558-018-0081-5.

129 Statistics New Zealand, 2015. Total Area of Farms, 2013., Statistics New Zealand, New Zealand.

130 Stevens, R.M., Ewenz, C.M., Grigson, G. and Conner, S.M., 2012. Water use by an irrigated almond
131 orchard. *Irrig. Sci.* 30: 189-200, DOI: 10.1007/s00271-011-0270-8.

132 Stokes, C.J., Howden, S.M., Gifford, R.G., Meinke, H., Bange, M., McRae, D., Roth, G., Gaydon, D.,
133 Beecher, H.G., Reinke, R., Crimp, S., Park, S., Inman-Bamber, G., Webb, L., Barlow, E.W.R.,
134 Hennessy, K., Whetton, P.H., Booth, T.H., Kirschbaum, M.U.F., Battaglia, M., Stone, G.,
135 Cobon, D., and Ash, A., McKeon, G., Miller, C.J., Jones, R.N., Hobday, A. J., and
136 Poloczanska, E. S., 2008. An overview of climate change adaptation in Australian primary
137 industries: impacts, options and priorities. Report prepared for the National Climate Change
138 Research Strategy for Primary Industries, CSIRO, Canberra, ACT, Australia.

139 Stoy, P.C., Katul, G.G., Siqueira, M.B.S., Juang, J.Y., McCarthy, H.R., Kim, H.S., Oishi, A.C. and
140 Oren, R., 2005. Variability in net ecosystem exchange from hourly to inter-annual time scales
141 at adjacent pine and hardwood forests: a wavelet analysis. *Tree Physiol.* 25: 887-902.

142 Stoy, P.C., Mauder, M., Foken, T., Marcolla, B., Boegh, E., Ibrom, A., Arain, M.A., Arneth, A.,
143 Aurela, M., Bernhofer, C., Cescatti, A., Dellwik, E., Duce, P., Gianelle, D., van Gorsel, E.,
144 Kiely, G., Knohl, A., Margolis, H., McCaughey, H., Merbold, L., Montagnani, L., Papale, D.,
145 Reichstein, M., Saunders, M., Serrano-Ortiz, P., Sottocornola, M., Spano, D., Vaccari, F. and
146 Varlagin, A., 2013. A data-driven analysis of energy balance closure across FLUXNET
147 research sites: The role of landscape scale heterogeneity. *Agric. For. Meteorol.* 171-172: 137-
148 152, DOI: 10.1016/j.agrformet.2012.11.004.

149 Stull, R.B., 1988. *An Introduction to Boundary Layer Meteorology*. Atmospheric Sciences Library.
150 Kluwer Academic Publishers, Boston, MA, 666 pp.

151 Tallec, T., Béziat, P., Jarosz, N., Rivalland, V. and Ceschia, E., 2013. Crops' water use efficiencies in
152 temperate climate: Comparison of stand, ecosystem and agronomical approaches. *Agric. For.*
153 *Meteorol.* 168: 69-81, DOI: 10.1016/j.agrformet.2012.07.008.

154 Thompson, M.A., Campbell, D.I. and Spronken-Smith, R.A., 1999. Evaporation from natural and
155 modified raised peat bogs in New Zealand. *Agric. For. Meteorol.* 95: 85-98, DOI:
156 10.1016/s0168-1923(99)00027-1.

157 Torrence, C. and Compo, G.P., 1998. A practical guide to wavelet analysis. *Bull. Amer. Meteor. Soc.*
158 79: 61-78.

159 Ummenhofer, C.C., Xu, H., Twine, T.E., Girvetz, E.H., McCarthy, H.R., Chhetri, N. and Nicholas,
160 K.A., 2015. How climate change affects extremes in maize and wheat yield in two cropping
161 regions. *J. Clim.* 28: 4653-4687, DOI: 10.1175/jcli-d-13-00326.1.

162 van Delden, L., Larsen, E., Rowlings, D., Scheer, C. and Grace, P., 2016. Establishing turf grass
163 increases soil greenhouse gas emissions in peri-urban environments. *Urban Ecosyst.*: 1-14,
164 DOI: 10.1007/s11252-016-0529-1.

165 van Dijk, A., Beck, H.E., Crosbie, R.S., de Jeu, R.A.M., Liu, Y.Y., Podger, G.M., Timbal, B. and
166 Viney, N.R., 2013. The Millennium Drought in southeast Australia (2001-2009): Natural and
167 human causes and implications for water resources, ecosystems, economy, and society. *Water*
168 *Resour. Res.* 49: 1040-1057, DOI: 10.1002/wrcr.20123.

169 van Gorsel, E., Berni, J.A.J., Briggs, P., Cabello-Leblic, A., Chasmer, L., Cleugh, H.A., Hacker, J.,
170 Hantson, S., Haverd, V., Hughes, D., Hopkinson, C., Keith, H., Kljun, N., Leuning, R., Yebra,
171 M. and Zegelin, S., 2013. Primary and secondary effects of climate variability on net
172 ecosystem carbon exchange in an evergreen *Eucalyptus* forest. *Agric. For. Meteorol.* 182-183:
173 248-256, DOI: 10.1016/j.agrformet.2013.04.027.

- 174 van Gorsel, E., Cleverly, J., Beringer, J., Cleugh, H., Eamus, D., Hutley, L.B., Isaac, P. and Prober, S.,
175 2018. Preface: Ozflux: a network for the study of ecosystem carbon and water dynamics
176 across Australia and New Zealand. *Biogeosciences*. 15: 349-352, DOI: 10.5194/bg-15-349-
177 2018.
- 178 van Gorsel, E., Wolf, S., Cleverly, J., Isaac, P., Haverd, V., Ewenz, C., Arndt, S., Beringer, J., Resco
179 de Dios, V., Evans, B.J., Griebel, A., Hutley, L.B., Keenan, T., Kljun, N., Macfarlane, C.,
180 Meyer, W.S., McHugh, I., Pendall, E., Prober, S.M. and Silberstein, R., 2016. Carbon uptake
181 and water use in woodlands and forests in southern Australia during an extreme heat wave
182 event in the “Angry Summer” of 2012/2013. *Biogeosciences*. 13: 5947-5964, DOI:
183 10.5194/bg-13-5947-2016.
- 184 van Heerwaarden, C.C. and Teuling, A.J., 2014. Disentangling the response of forest and grassland
185 energy exchange to heatwaves under idealized land-atmosphere coupling. *Biogeosciences*. 11:
186 6159-6171, DOI: 10.5194/bg-11-6159-2014.
- 187 Vote, C., Hall, A. and Charlton, P., 2015. Carbon dioxide, water and energy fluxes of irrigated broad-
188 acre crops in an Australian semi-arid climate zone. *Environmental Earth Sciences*. 73: 449-465,
189 DOI: 10.1007/s12665-014-3547-4.
- 190 Wagle, P., Gowda, P.H., Anapalli, S.S., Reddy, K.N. and Northup, B.K., 2017a. Growing season
191 variability in carbon dioxide exchange of irrigated and rainfed soybean in the southern United
192 States. *Sci. Total Environ*. 593: 263-273, DOI: 10.1016/j.scitotenv.2017.03.163.
- 193 Wagle, P., Xiao, X.M., Gowda, P., Basara, J., Brunzell, N., Steiner, J. and Anup, K.C., 2017b.
194 Analysis and estimation of tallgrass prairie evapotranspiration in the central United States.
195 *Agric. For. Meteorol*. 232: 35-47, DOI: 10.1016/j.agrformet.2016.08.005.
- 196 Waldo, S., Chi, J., Pressley, S.N., O’Keeffe, P., Pan, W.L., Brooks, E.S., Huggins, D.R., Stöckle, C.O.
197 and Lamb, B.K., 2016. Assessing carbon dynamics at high and low rainfall agricultural sites in
198 the inland Pacific Northwest US using the eddy covariance method. *Agric. For. Meteorol*. 218–
199 219: 25-36, DOI: 10.1016/j.agrformet.2015.11.018.
- 200 Wang, L., Liu, H.Z. and Bernhofer, C., 2017. Response of carbon dioxide exchange to grazing
201 intensity over typical steppes in a semi-arid area of Inner Mongolia. *Theor. Appl. Climatol*.
202 128: 719-730, DOI: 10.1007/s00704-016-1736-7.
- 203 Waters, C.M., Orgill, S.E., Melville, G.J., Toole, I.D. and Smith, W.J., 2017. Management of Grazing
204 Intensity in the Semi-Arid Rangelands of Southern Australia: Effects on Soil and Biodiversity.
205 *Land Degrad. Dev*. 28: 1363-1375, DOI: 10.1002/ldr.2602.
- 206 Webb, J.R., Santos, I.R., Maher, D.T., Macdonald, B., Robson, B., Isaac, P. and McHugh, I., 2018.
207 Terrestrial versus aquatic carbon fluxes in a subtropical agricultural floodplain over an annual
208 cycle. *Agric. For. Meteorol*. 260-261: 262-272, DOI: 10.1016/j.agrformet.2018.06.015.
- 209 Whitehead, D., Schipper, L.A., Pronger, J., Moinet, G.Y.K., Mudge, P.L., Calvelo Pereira, R.,
210 Kirschbaum, M.U.F., McNally, S.R., Beare, M.H. and Camps-Arbestain, M., 2018.
211 Management practices to reduce losses or increase soil carbon stocks in temperate grazed
212 grasslands: New Zealand as a case study. *Agric. Ecosyst. Environ*. 265: 432-443, DOI:
213 10.1016/j.agee.2018.06.022.
- 214 Whitley, R.J., Macinnis-Ng, C.M.O., Hutley, L.B., Beringer, J., Zeppel, M., Williams, M., Taylor, D.
215 and Eamus, D., 2011. Is productivity of mesic savannas light limited or water limited? Results
216 of a simulation study. *Glob. Change Biol*. 17: 3130–3149, DOI: 10.1111/j.1365-
217 2486.2011.02425.x.

218 Williams, J., Hook, R.A. and Hamblin, A., 2002. Agro-ecological regions of Australia: Methodologies
 219 for their derivation and key issues in resource management, CSIRO Land and Water, Canberra,
 220 ACT, Australia.

221 Xie, Z., Huete, A., Cleverly, J., Phinn, S., McDonald-Madden, E., Cao, Y. and Qin, F., 2019. Multi-
 222 climate mode interactions drive hydrological and vegetation responses to hydroclimatic
 223 extremes in Australia. *Remote Sens. Environ.* 231: 111270, DOI: 10.1016/j.rse.2019.111270.

224 Yang, Z., Dominguez, F., Zeng, X.B., Hu, H.C., Gupta, H. and Yang, B., 2017. Impact of irrigation
 225 over the California Central Valley on regional climate. *J. Hydrometeor.* 18: 1341-1357.

226 Zeeman, M.J., Hiller, R., Gilgen, A.K., Michna, P., Pluss, P., Buchmann, N. and Eugster, W., 2010.
 227 Management and climate impacts on net CO₂ fluxes and carbon budgets of three grasslands
 228 along an elevational gradient in Switzerland. *Agric. For. Meteorol.* 150: 519-530, DOI:
 229 10.1016/j.agrformet.2010.01.011.

230 Zhang, Y.Q., Chiew, F.H.S., Pena-Arancibia, J., Sun, F.B., Li, H.X. and Leuning, R., 2017. Global
 231 variation of transpiration and soil evaporation and the role of their major climate drivers. *J.*
 232 *Geophys. Res.: Atmos.* 122: 6868-6881, DOI: 10.1002/2017jd027025.

233 Zhou, Y.T., Xiao, X.M., Wagle, P., Bajgain, R., Mahan, H., Basara, J.B., Dong, J.W., Qin, Y.W.,
 234 Zhang, G.L., Luo, Y.Q., Gowda, P.H., Neel, J.P.S., Starks, P.J. and Steiner, J.L., 2017.
 235 Examining the short-term impacts of diverse management practices on plant phenology and
 236 carbon fluxes of Old World bluestems pasture. *Agric. For. Meteorol.* 237: 60-70, DOI:
 237 10.1016/j.agrformet.2017.01.018.

238 Zscheischler, J., Fatichi, S., Wolf, S., Blanken, P.D., Bohrer, G., Clark, K., Desai, A.R., Hollinger, D.,
 239 Keenan, T., Novick, K.A. and Seneviratne, S.I., 2016. Short-term favorable weather conditions
 240 are an important control of interannual variability in carbon and water fluxes. *J. Geophys. Res.:*
 241 *Biogeosci.* 121: 2186-2198, DOI: 10.1002/2016JG003503.